ESAIM: M2AN
Vol. 38, N° 6, 2004, pp. 903–929
DOI: 10.1051/m2an:2004044

ESAIM: Mathematical Modelling and Numerical Analysis

RESIDUAL AND HIERARCHICAL *A POSTERIORI* ERROR ESTIMATES FOR NONCONFORMING MIXED FINITE ELEMENT METHODS

Linda El Alaoui[1] and Alexandre Ern[1]

Abstract. We analyze residual and hierarchical *a posteriori* error estimates for nonconforming finite element approximations of elliptic problems with variable coefficients. We consider a finite volume box scheme equivalent to a nonconforming mixed finite element method in a Petrov–Galerkin setting. We prove that all the estimators yield global upper and local lower bounds for the discretization error. Finally, we present results illustrating the efficiency of the estimators, for instance, in the simulation of Darcy flows through heterogeneous porous media.

Mathematics Subject Classification. 65N15, 65N60, 75N12, 76905.

Received June 22, 2003.

1. Introduction

Detailed simulation of advective, diffusive, and dispersive transport of pollutants in soils requires an accurate description of the flow field. A widely used model for steady subsurface flows in saturated porous media consists of Darcy's equations

$$\begin{cases} \sigma + k\,\nabla u = 0, \\ \nabla{\cdot}\sigma = f, \end{cases} \tag{1.1}$$

where σ is the velocity vector, k the hydraulic conductivity, u the hydraulic head (or the pressure up to an appropriate rescaling), and f the source term resulting from mass sources or sinks. The first equation in (1.1) is Darcy's phenomenological law and the second equation expresses mass conservation. Problem (1.1) is posed on a domain Ω and is completed by flux or head conditions on the boundary $\partial\Omega$. Elimination of the velocity yields the elliptic equation

$$-\nabla{\cdot}(k\,\nabla u) = f. \tag{1.2}$$

Equations (1.1) and (1.2) arise in many other elliptic models, (1.1) providing a mixed formulation of (1.2).

Problem (1.1) can be cast into several weak formulations. On the one hand, one can consider two symmetric formulations in which the solution space for the unknowns (σ, u) is the same as the test space. The two formulations differ from the fact that either the velocity or the pressure is sought in a space with more regularity. On the other hand, it is also possible to consider nonsymmetric formulations in which the solution and test spaces are different. The present work focuses on one of such formulations, in which both velocity and pressure solution

Keywords and phrases. Finite elements, nonconforming methods, *a posteriori* error estimates, finite volumes, Darcy equations, heterogeneous media.

[1] CERMICS, École nationale des ponts et chaussées, 6 et 8, avenue Blaise Pascal, 77455 Marne la Vallée Cedex 2, France. e-mail: {elalaoui,ern}@cermics.enpc.fr

spaces have more regularity than the corresponding test spaces [16, 17, 30]. Assuming for the sake of simplicity that homogeneous Dirichlet boundary conditions are enforced on the pressure and, as is usual in *a posteriori* error analysis, that the data f is in $L^2(\Omega)$, consider the following weak formulation of (1.1)

$$\begin{cases} \text{Find } (\sigma, u) \in H(\mathrm{div};\Omega) \times H_0^1(\Omega) \text{ such that} \\ \displaystyle\int_\Omega \sigma\cdot\tau + \int_\Omega k\,\tau\cdot\nabla u = 0 \qquad \forall\, \tau \in [L^2(\Omega)]^d, \\ \displaystyle\int_\Omega v\,\nabla\cdot\sigma = \int_\Omega fv \qquad\qquad \forall\, v \in L^2(\Omega), \end{cases} \tag{1.3}$$

where $H(\mathrm{div};\Omega) = \{\, \sigma \in [L^2(\Omega)]^d,\ \nabla\cdot\sigma \in L^2(\Omega) \,\}$ and d is the space dimension. Flux boundary conditions can be incorporated by considering an appropriate subspace of $H(\mathrm{div};\Omega)$. Elimination of the velocity yields the following weak formulation of (1.2)

$$\begin{cases} \text{Find } u \in H_0^1(\Omega) \text{ such that} \\ \displaystyle\int_\Omega k\,\nabla u\cdot\nabla v = \int_\Omega fv \qquad \forall\, v \in H_0^1(\Omega). \end{cases} \tag{1.4}$$

The weak formulation (1.3) is attractive because it can be approximated by a mixed finite element method of Petrov–Galerkin type in which the discrete test functions are localized at the mesh cells. Therefore, the discrete scheme can be interpreted as a finite volume method, often termed finite volume box scheme. For Darcy's equations, the lowest-order finite volume box scheme has been introduced in [16] and further investigated in [17], while higher-order versions have been analyzed in [18]. Finite volume box schemes are endowed with two important properties, both holding at the cell level: mass conservation and an explicit velocity reconstruction formula. To achieve these properties, the Petrov–Galerkin mixed finite element method has to be set in a *nonconforming* framework. For instance, in the lowest-order finite volume box scheme, the pressure is approximated in the Crouzeix–Raviart finite element space.

The main goal of this work is to derive *a posteriori* error estimates yielding global upper bounds and local lower bounds for approximations of (1.3) based on the lowest-order finite volume box scheme. This entails, in particular, to perform the *a posteriori* error analysis in a nonconforming framework. Global upper bounds are important for reliability issues while local lower bounds lead to error indicators that can be used to refine the mesh adaptively. Owing to its aforementioned advantages, the finite volume box scheme appears to be a very promising method to simulate accurately Darcy's equations, but only its *a priori* error analysis is so far available in the literature, thus preventing its implementation together with adaptive mesh strategies. Furthermore, nonconforming finite element methods are attractive on their own since they yield a more compact stencil than the conforming methods, a feature that simplifies communications when parallelizing the method.

We investigate residual and hierarchical techniques to derive *a posteriori* error estimates. For a thorough introduction to these techniques in the framework of conforming finite element methods, see [5, 32] and references therein. *A posteriori* error estimates for nonconforming and mixed finite element approximations of the Poisson, Darcy, and Stokes equations have experienced a significant development over the last decade; see, among others, [2, 4, 6, 10, 14, 20, 21, 24–27, 29, 31, 33]. *A posteriori* error estimates for nonconforming finite elements entail additional terms with respect to the conforming case. These terms can be the jumps across element interfaces of tangential derivatives of the finite element solution [15, 20, 21], or the jump of the finite element solution itself [4, 25, 29]; alternatively, local subproblems can be considered to evaluate these terms [24]. Recently, an abstract framework for a posteriori error estimates with violated Galerkin orthogonality has been introduced [6], leading to estimates involving the difference between the nonconforming finite element solution and a conforming approximation thereof [29]. For Darcy's equations, similar techniques have been employed in [4] where both conforming and nonconforming finite element approximations of the symmetric formulation of (1.1) are addressed. In practice, the conforming reconstruction of the discrete solution often uses an interpolation operator introduced by Oswald (see [4, 24]), an idea which we also employ hereafter. One original contribution of this work is to extend the analysis presented in [4] to the non-symmetric formulation of (1.1) associated with the lowest-order finite volume box scheme.

Hierarchical *a posteriori* error estimates have been introduced in [8, 9]. The analysis relies on a saturation assumption and a strengthened Cauchy–Schwarz inequality. The extension of these techniques to mixed formulations has been investigated in [2]. Application to Darcy's equations only includes the symmetric formulation of the problem with a more regular velocity space discretized by conforming Raviart–Thomas finite elements [2, 33]. Since the saturation assumption is generally difficult to assert and may even not hold, there is a clear motivation to derive hierarchical error estimates circumventing this assumption. Techniques achieving this goal in a conforming setting have been presented in [1]. A second original contribution of this work is to extend these techniques to a nonconforming setting.

Another relatively novel feature of this work is to address the case of variable coefficient k in (1.3). For strongly heterogeneous media, it is important that the constants arising in the *a posteriori* error estimates be independent of the fluctuations of k. To this purpose, we extend the work of [12] where appropriate norms are introduced for the *a priori* and the *a posteriori* analysis of (1.2) in a conforming setting.

This paper is organized as follows. The well-posedness of (1.3) and the *a priori* error analysis of the finite volume box scheme are presented in Section 2. Residual *a posteriori* error estimates are investigated in Section 3. Two estimators are derived, one based on the mixed formulation and one based on an equivalent primal formulation for the discrete pressure. Hierarchical *a posteriori* estimates are analyzed in Section 4. Estimators using conforming face bubbles and nonconforming element bubbles are considered. Numerical results are presented in Section 5. Conclusions are drawn in Section 6.

2. Well-posedness and *a priori* error analysis

In this section we discuss our model assumptions and establish the well-posedness of (1.3). We then describe the finite volume box scheme discretizing (1.3) and present its *a priori* error analysis.

2.1. Model assumptions and well-posedness

Let Ω be a bounded polygonal domain in $\mathbb{R}^d$ with $d = 2$ or 3. For the sake of simplicity, we restrict our analysis to isotropic media in which the hydraulic conductivity k is a scalar. However, we address the case of heterogeneous media in which k undergoes sharp variations in Ω. Since the hydraulic conductivity results from the geological properties of the medium, it is reasonable to make the following assumption:

Hypothesis 2.1. *There exists a partition $\overline{\Omega} = \bigcup_{l=1}^{L} \overline{\Omega}_l$ with $\Omega_l \cap \Omega_{l'} = \emptyset$ for $l \neq l'$, such that k equals a positive constant k_l in each Ω_l.*

This hypothesis will always be made implicitly in the rest of this work; it has also been used in [3, 12].

For strongly heterogeneous media, the condition ratio of k evaluated as $\varrho_\Omega(k) = \max_\Omega k / \min_\Omega k$ is very large. In practice, it is important that the constants arising in the error estimates be independent of this ratio. To this purpose, appropriate norms must be introduced to measure the error [12]. For a region R and $\varphi \in L^2(R)$, let $\|\varphi\|_{0,R}$ denote the L^2-norm of φ on R and also introduce $\|\varphi\|_{k^{\pm 1};0,R} = \|k^{\pm\frac{1}{2}}\varphi\|_{0,R}$. For conciseness, the same notation is used if φ is a vector-valued function in $[L^2(R)]^d$. The usual scalar product on $L^2(R)$ is denoted by $(\cdot,\cdot)_{0,R}$. For $\varphi \in H^m(R)$, $m = 1, 2$, let $|\varphi|_{m,R}$ denote the H^m-seminorm of φ over R. For $\varphi \in H^1(R)$, set $|\varphi|_{k;1,R} = \|k^{\frac{1}{2}}\nabla\varphi\|_{0,R}$. Finally, for $\psi \in H(\mathrm{div}; R)$, set $\|\psi\|_{k^{-1};\mathrm{div},R} = \|\psi\|_{k^{-1};0,R} + \|\nabla\cdot\psi\|_{k^{-1};0,R}$.

Set $V = H(\mathrm{div};\Omega) \times H_0^1(\Omega)$ and $W = [L^2(\Omega)]^d \times L^2(\Omega)$, equipped respectively with the norms

$$\|(\sigma, u)\|_V = \|\sigma\|_{k^{-1};\mathrm{div},\Omega} + |u|_{k;1,\Omega} \quad \text{and} \quad \|(\tau, v)\|_W = \|\tau\|_{k;0,\Omega} + \|v\|_{k;0,\Omega}. \tag{2.1}$$

Let $B(\cdot,\cdot)$ be the bilinear form defined on $V \times W$ by

$$B((\sigma, u), (\tau, v)) = (\sigma, \tau)_{0,\Omega} + (v, \nabla\cdot\sigma)_{0,\Omega} + (k\nabla u, \tau)_{0,\Omega}. \tag{2.2}$$

Proposition 2.2. *The problem* (1.3) *is well-posed.*

Proof. Owing to the Banach–Nečas–Babuška theorem (see, *e.g.*, [22], p. 85), the problem (1.3) is well-posed if and only if the two following conditions hold:

$$\exists \alpha > 0, \quad \inf_{(\sigma,u)\in V} \sup_{(\tau,v)\in W} \frac{B((\sigma,u),(\tau,v))}{\|(\sigma,u)\|_V \|(\tau,v)\|_W} \geq \alpha, \tag{BNB1}$$

$$\forall (\tau,v) \in W, \quad \{\forall (\sigma,u) \in V,\ B((\sigma,u),(\tau,v)) = 0\} \Rightarrow \{(\tau,v) = 0\}. \tag{BNB2}$$

Proof of (BNB1). Set $(\tau,v) = (k^{-1}\sigma + \nabla u, 2u + k^{-1}\nabla\cdot\sigma)$. Then,

$$B((\sigma,u),(\tau,v)) = \int_\Omega (k^{-1}|\sigma|^2 + k|\nabla u|^2 + k^{-1}|\nabla\cdot\sigma|^2 + 2\sigma\cdot\nabla u + 2u\nabla\cdot\sigma) = \|(\sigma,u)\|_V^2,$$

since $\int_\Omega \sigma\cdot\nabla u + u\nabla\cdot\sigma = 0$. Let C_Ω be the Poincaré constant such that for all $u \in H_0^1(\Omega)$, $\|u\|_{0,\Omega} \leq C_\Omega \|\nabla u\|_{0,\Omega}$. Then, for all $u \in H_0^1(\Omega)$, $\|k^{\frac12} u\|_{0,\Omega} \leq C_\Omega \varrho_\Omega(k)^{\frac12} \|k^{\frac12}\nabla u\|_{0,\Omega}$, and hence,

$$\|(\tau,v)\|_W^2 \leq 4(\|\sigma\|_{k^{-1};\mathrm{div},\Omega}^2 + 4\|u\|_{k;0,\Omega}^2 + \|\nabla u\|_{k;0,\Omega}^2) \leq 4(\|(\sigma,u)\|_V^2 + 4C_\Omega^2 \varrho_\Omega(k)|u|_{k;1,\Omega}^2).$$

Thus, the inf-sup condition (BNB1) holds with $\alpha^{-1} = 2(1 + 4C_\Omega^2 \varrho_\Omega(k))^{\frac12}$.

Proof of (BNB2). Let $(\tau,v) \in W$ be such that (BNB1) holds. Let $\widehat{v} \in H_0^1(\Omega)$ be the unique solution of $\nabla\cdot k\nabla\widehat{v} = v$. Then setting $(\sigma,u) = (-k\nabla\widehat{v}, \widehat{v})$, it is clear that $(\sigma,u) \in V$ and

$$0 = B((\sigma,u),(\tau,v)) = \int_\Omega \sigma\cdot\tau + k\tau\cdot\nabla u + v\nabla\cdot\sigma = -\int_\Omega v^2,$$

which implies $v = 0$. Finally, taking $(\sigma,u) = (\tau,0)$ yields $\tau = 0$. □

Remark 2.3. Since $\varrho_\Omega(k) \geq 1$, the constant α in (BNB1) can always be lower bounded in the form $\alpha \geq c\varrho_\Omega(k)^{-\frac12}$ with c independent of k.

2.2. The finite volume box scheme

Let $(\mathcal{T}_h)_h$ be a shape-regular family of triangulations of Ω (it is implicitly understood that in three dimensions, triangles should be replaced by tetrahedra). In the sequel, we will always make the following assumption:

Hypothesis 2.4. *For all h, the triangulation $\mathcal{T}_h$ is compatible with the partition $\overline{\Omega} = \cup_{l=1}^L \overline{\Omega}_l$ in the sense that the interior of any triangle $T \in \mathcal{T}_h$ has a nonempty intersection with only one of the subdomains Ω_l.*

Let $H^1(\mathcal{T}_h) = \{v \in L^2(\Omega)\,; \forall T \in \mathcal{T}_h,\ v|_T \in H^1(T)\}$. For a triangle $T \in \mathcal{T}_h$, let h_T be its diameter and set $h = \max_{T\in\mathcal{T}_h} h_T$. Let $\mathcal{F}_h$, $\mathcal{F}_h^i$, and $\mathcal{F}_h^\partial$ denote respectively the set of faces, internal, and external faces in $\mathcal{T}_h$. For a face $F \in \mathcal{F}_h$, let h_F be its diameter and let $\mathcal{T}_F$ be the set of elements in $\mathcal{T}_h$ containing F. For an element $T \in \mathcal{T}_h$, let $\mathcal{F}_T$ be the set of faces belonging to T. For $F \in \mathcal{F}_h$, choose a unit normal vector n_F. For a piecewise continuous function φ on $\mathcal{T}_h$, $[\varphi]_F$ denotes the jump of φ across F in the direction of n_F, with the convention that a zero outer value is taken for faces contained in $\partial\Omega$. The arbitrariness in the sign of $[\varphi]_F$ is irrelevant in the analysis below.

Owing to Hypotheses 2.1 and 2.4, the coefficient k is constant on T and its local value will be denoted by k_T. For $F \in \mathcal{F}_h^i$, such that $F = T \cap T'$ with T and T' in $\mathcal{T}_h$, set $\{k\}_F = \frac12(k_T + k_{T'})$, $k_F^\star = \max(k_T, k_{T'})$, and $\varrho_F(k) = \max(k_T, k_{T'})/\min(k_T, k_{T'})$. For $F \in \mathcal{F}_h^\partial$, with $F \in \mathcal{F}_T$, set $\{k\}_F = k_T$ and $\varrho_F(k) = 1$. Finally, c always denotes a generic positive constant which neither depends on h nor on the ratios $\varrho_\Omega(k)$ and $\varrho_F(k)$ for all $F \in \mathcal{F}_h$ (the value of c can change at each occurrence).

We seek the discrete velocity in the $H(\mathrm{div};\Omega)$-conforming Raviart–Thomas finite element space $RT^0(\mathcal{T}_h)$ of lowest-order [28] and the discrete pressure in the nonconforming Crouzeix–Raviart finite element space [19]

$$P^1_{\mathrm{nc},0}(\mathcal{T}_h) = \{\, v_h \in L^2(\Omega);\ \forall T \in \mathcal{T}_h,\ v_h|_T \in P^1(T);\ \forall F \in \mathcal{F}_h,\ \int_F [v_h]_F = 0 \,\}, \tag{2.3}$$

where $P^1(T)$ is the space of polynomials on T with degree ≤ 1. The test functions for the pressure and the velocity are taken to be piecewise constant. Let $P^0(\mathcal{T}_h)$ be the space spanned by (scalar-valued) piecewise constant functions on $\mathcal{T}_h$. The nonconforming mixed finite element discretization of (1.3) corresponds to the finite volume box scheme

$$\begin{cases} \text{Find } (\sigma_h, u_h) \in RT^0(\mathcal{T}_h) \times P^1_{\mathrm{nc},0}(\mathcal{T}_h) \text{ such that} \\ a(\sigma_h, \tau_h) + b_{1,h}(\tau_h, u_h) = 0 \qquad \forall\, \tau_h \in [P^0(\mathcal{T}_h)]^d, \\ b_2(\sigma_h, v_h) = (f, v_h)_{0,\Omega} \qquad \forall\, v_h \in P^0(\mathcal{T}_h), \end{cases} \tag{2.4}$$

with the bilinear forms

$$a(\sigma_h, \tau_h) = (\sigma_h, \tau_h)_{0,\Omega}, \quad b_{1,h}(\tau_h, u_h) = \sum_{T \in \mathcal{T}_h} k_T (\tau_h, \nabla u_h)_{0,T}, \quad b_2(\sigma_h, v_h) = (\nabla\cdot\sigma_h, v_h)_{0,\Omega}. \tag{2.5}$$

The well-posedness of (2.4) can be established as in [17] for constant coefficient k. Following similar arguments, it is easily shown that the discrete problem (2.4) is well-posed for variable coefficient k. Alternatively, the well-posedness can be established by proving a discrete inf-sup condition; see ([22], p. 273) for the proof with constant coefficient k. Furthermore, it is straightforward to verify [17] that the discrete pressure u_h is also the unique solution of the problem

$$\begin{cases} \text{Find } u_h \in P^1_{\mathrm{nc},0}(\mathcal{T}_h) \text{ such that} \\ \Lambda_h(u_h, v_h) = (f_h, v_h)_{0,\Omega} \quad \forall v_h \in P^1_{\mathrm{nc},0}(\mathcal{T}_h), \end{cases} \tag{2.6}$$

with

$$\Lambda_h(u_h, v_h) = \sum_{T \in \mathcal{T}_h} k_T (\nabla u_h, \nabla v_h)_{0,T}, \tag{2.7}$$

and $f_h = \Pi^0 f$ where Π^0 denotes the orthogonal projector from $L^2(\Omega)$ onto $P^0(\mathcal{T}_h)$. Problem (2.6) will be termed the "primal formulation".

Two important properties satisfied by the solution of (2.4) are the following:

- The discrete velocity σ_h can be reconstructed locally from the expression

$$\forall T \in \mathcal{T}_h, \quad \sigma_h|_T = -k_T \nabla u_h|_T + \frac{1}{d}(f_h \pi_h^1)|_T, \tag{2.8}$$

  where π_h^1 is a piecewise first-order polynomial such that for all $T \in \mathcal{T}_h$ and for all $x = (x_1, \cdots, x_d) \in T$, $\pi_h^1(x) = (x_1 - G_{T,1}, \cdots, x_d - G_{T,d})$, $(G_{T,1}, \ldots, G_{T,d})$ being the coordinates of the center of mass of T. For further use, introduce the gyration radius of T, $\rho_T = |T|^{-\frac{1}{2}} \|\pi_h^1\|_{0,T}$, where $|T|$ is the d-measure of T. The property (2.8) is closely related to the fact that the finite volume box scheme coincides with one of the post-processings of the classical mixed method discussed in [7].
- The discrete velocity σ_h satisfies the mass conservation equation

$$\nabla\cdot\sigma_h = f_h. \tag{2.9}$$

2.3. *A priori* error analysis

For $v \in H_0^1(\Omega) + P^1_{\mathrm{nc},0}(\mathcal{T}_h)$, introduce the broken energy norm

$$|v|_{k;1,h} = \left(\sum_{T\in\mathcal{T}_h} |v|^2_{k;1,T} \right)^{\frac{1}{2}}. \tag{2.10}$$

Proposition 2.5. *Let* (σ, u) *and* (σ_h, u_h) *be respectively the unique solution of* (1.3) *and* (2.4). *Assume* $u|_T \in H^2(T)$ *for all* $T \in \mathcal{T}_h$. *Then, there exists a constant* c *such that*

$$c|u-u_h|_{k;1,h} \leq \left(\sum_{T\in\mathcal{T}_h} h_T^2 k_T |u|^2_{2,T} \right)^{\frac{1}{2}} + h\|f-f_h\|_{k^{-1};0,\Omega}, \tag{2.11}$$

$$c\|\sigma-\sigma_h\|_{k^{-1};0,\Omega} \leq |u-u_h|_{k;1,h} + h\|f_h\|_{k^{-1};0,\Omega}. \tag{2.12}$$

Proof. The proof is similar to the one presented in [16] for constant coefficient k and we only highlight the differences when k is variable. Since u_h solves the nonconforming finite element problem (2.6), we deduce using classical techniques (see for instance [22]) that

$$|u-u_h|_{k;1,h} \leq 2 \inf_{w_h\in P^1_{\mathrm{nc},0}(\mathcal{T}_h)} |u-w_h|_{k;1,h} + \sup_{v_h\in P^1_{\mathrm{nc},0}(\mathcal{T}_h)} \frac{(f_h,v_h)_{0,\Omega} - \Lambda_h(u,v_h)}{|v_h|_{k;1,h}}.$$

Using standard interpolation techniques locally on each element T, the first term in the right-hand side can be estimated in the form $c\left(\sum_{T\in\mathcal{T}_h} h_T^2 k_T |u|^2_{2,T}\right)^{\frac{1}{2}}$. Concerning the second term, an integration by parts yields

$$(f_h,v_h)_{0,\Omega} - \Lambda_h(u,v_h) = -(f-f_h,v_h)_{0,\Omega} - \sum_{T\in\mathcal{T}_h} k_T \int_{\partial T} \partial_n u\, v_h.$$

The first term in the right-hand side is readily estimated as

$$(f-f_h,v_h)_{0,\Omega} = (f-f_h, v_h - \Pi^0 v_h)_{0,\Omega} \leq \|f-f_h\|_{k^{-1};0,\Omega}\|v_h-\Pi^0 v_h\|_{k;0,\Omega} \leq ch\|f-f_h\|_{k^{-1};0,\Omega}|v_h|_{k;1,h},$$

whereas classical interpolation techniques (see for instance [13], p. 110) yield for the second term

$$\sum_{T\in\mathcal{T}_h} k_T \int_{\partial T} \partial_n u\, v_h \leq c \left(\sum_{T\in\mathcal{T}_h} h_T^2 k_T |u|^2_{2,T} \right)^{\frac{1}{2}} |v_h|_{k;1,h}.$$

Combining the above estimates yields (2.11). Finally, (2.12) directly follows from (2.8). □

Remark 2.6. Without any additional regularity assumption on f, the only estimate available for the divergence of the velocity is $\|\nabla\cdot(\sigma-\sigma_h)\|_{k^{-1};0,\Omega} \leq \|f-f_h\|_{k^{-1};0,\Omega}$. Therefore, although $\|\sigma-\sigma_h\|_{k^{-1};0,\Omega}$ converges to first-order in h owing to (2.12), the same conclusion does not necessarily hold for $\|\sigma-\sigma_h\|_{k^{-1};\mathrm{div},\Omega}$. In most applications, it is reasonable to assume that the data has more regularity. For instance, if $f \in H^1(\mathcal{T}_h)$, first-order convergence in the V-norm is achieved.

Remark 2.7. The *a priori* error analysis of (2.4) can also be performed in the spirit of the Second Strang Lemma by considering the mixed formulation. The analysis can be derived by extending that of ([22], p. 273) to the case of variable conductivity. If f is only in $L^2(\Omega)$, the Raviart–Thomas finite element space does not yield any approximability property on $\nabla\cdot\sigma$ and hence, it is not possible to infer that the error converges to zero in the V-norm. If $f \in H^1(\mathcal{T}_h)$, the analysis yields first-order convergence in the V-norm.

3. Residual *a posteriori* error analysis

In this section we analyze two residual *a posteriori* error estimators. The first estimator is obtained from the mixed formulation (2.4) and the second from the primal formulation (2.6). The first presents the drawback that the constants arising in the estimate depend on the ratio $\varrho_\Omega(k)$, whereas the second yields constants independent of this ratio. The numerical experiments presented in Section 5 for strongly heterogeneous media show that both estimators can retain their usefulness.

3.1. **Preliminary results**

Let $P^1_{\mathrm{c},0}(\mathcal{T}_h) = P^1_{\mathrm{nc},0}(\mathcal{T}_h) \cap H^1_0(\Omega)$ be the conforming finite element space of degree one. In the sequel, our analysis will rely on the following hypothesis which is inspired from that introduced in ([12], p. 590).

Hypothesis 3.1. *For all pairs of elements in $\mathcal{T}_h$ sharing a vertex, there exists a path through adjacent elements (adjacent means that the elements share a face) such that all the elements share the vertex in question and such that the function k is monotone along this path.*

In dimension 2, a sufficient condition for Hypothesis 3.1 to hold is that there are at most three subdomains sharing a common point in Ω and at most two subdomains sharing a common point on $\partial\Omega$. Clearly, it is straightforward to construct a counterexample to Hypothesis 3.1 using four subdomains; hence, one cannot claim that this hypothesis holds in all practical situations. This hypothesis is needed to construct interpolation operators yielding approximation properties that are uniform in the hydraulic conductivity.

- Under Hypothesis 3.1, it is proven in [12], Lemma 2.8, that there exists an interpolation operator $\mathcal{I}_{\mathrm{BV}} : L^2(\Omega) \to P^1_{\mathrm{c},0}(\mathcal{T}_h)$ such that

$$\forall v \in H^1_0(\Omega), \quad \forall T \in \mathcal{T}_h, \quad \|v - \mathcal{I}_{\mathrm{BV}} v\|_{0,T} \le c h_T (k_T)^{-\frac{1}{2}} |v|_{k;1,\Delta_T}, \tag{3.1}$$

$$\forall v \in H^1_0(\Omega), \quad \forall F \in \mathcal{F}^i_h, \quad \|v - \mathcal{I}_{\mathrm{BV}} v\|_{0,F} \le c h_F^{\frac{1}{2}} (k_F^\star)^{-\frac{1}{2}} |v|_{k;1,\Delta_F}, \tag{3.2}$$

  where Δ_T and Δ_F denote the union of all the elements in $\mathcal{T}_h$ that share at least one vertex with T and F respectively, and where $|v|^2_{k;1,\Delta_T} = \sum_{T\in\Delta_T} \|\nabla v\|^2_{k;0,T}$ and $|v|^2_{k;1,\Delta_F} = \sum_{T\in\Delta_F} \|\nabla v\|^2_{k;0,T}$.
- Let $\mathcal{I}_{\mathrm{Os}} : P^1_{\mathrm{nc},0}(\mathcal{T}_h) \to P^1_{\mathrm{c},0}(\mathcal{T}_h)$ be the Oswald interpolation operator defined for v_h in $P^1_{\mathrm{nc},0}(\mathcal{T}_h)$ as the unique function in $P^1_{\mathrm{c},0}(\mathcal{T}_h)$ such that for all interior vertex $s \in \mathcal{V}^i_h$,

$$\mathcal{I}_{\mathrm{Os}} v_h(s) = \frac{1}{\sharp(\mathcal{T}_s)} \sum_{T\in\mathcal{T}_s} v_h|_T(s), \tag{3.3}$$

  where $\mathcal{V}^i_h$ is the set of interior vertices in the mesh, $\mathcal{T}_s$ the set of elements in $\mathcal{T}_h$ containing s, and $\sharp(\mathcal{T}_s)$ the cardinal of this set. The Oswald interpolation operator has been considered in [4, 24, 27]. Under Hypothesis 3.1, there exists a constant c such that

$$\forall v_h \in P^1_{\mathrm{nc},0}(\mathcal{T}_h),\ \forall T \in \mathcal{T}_h, \quad |v_h - \mathcal{I}_{\mathrm{Os}} v_h|_{k;1,T} \le c \left(\sum_{F\in\mathcal{F}^{\mathrm{Os}}_T} \{k\}_F h_F^{-1} \|[v_h]_F\|^2_{0,F} \right)^{\frac{1}{2}}, \tag{3.4}$$

  where $\mathcal{F}^{\mathrm{Os}}_T$ denotes all the faces in the mesh containing a vertex of T. When Dirichlet conditions are not enforced, the upper bound in (3.4) does not include boundary faces; see [11] for a proof. In the present case, the proof is similar but the upper bound must include boundary faces.

3.2. Estimator based on the mixed formulation

Proposition 3.2. *Let* (σ, u) *and* (σ_h, u_h) *be respectively the unique solution of* (1.3) *and* (2.4). *Then, there exists a constant* c *such that*

$$|u-u_h|_{k;1,h} + \|\sigma-\sigma_h\|_{k^{-1};\mathrm{div},\Omega} \le c\varrho_\Omega(k)^{\frac{1}{2}} \left(\sum_{T\in\mathcal{T}_h} \mathcal{P}_{1,T}(f)^2 + \inf_{v_h\in P^1_{c,0}(\mathcal{T}_h)} |u_h - v_h|^2_{k;1,h} \right)^{\frac{1}{2}}, \qquad (3.5)$$

where we have introduced the local error indicators

$$\forall T\in\mathcal{T}_h, \quad \mathcal{P}_{1,T}(f) = \|f-f_h\|_{k^{-1};0,T} + \frac{1}{d}\rho_T\|f_h\|_{k^{-1};0,T}. \qquad (3.6)$$

Proof. Let v_h be an arbitrary function in $P^1_{c,0}(\mathcal{T}_h)$ and let $\sigma_h \in RT^0(\mathcal{T}_h)$ be the discrete velocity field from the solution of (2.4). Since $(\sigma, u) \in H(\mathrm{div};\Omega)\times H^1_0(\Omega)$ solves (1.3), for all $(\tau, v)\in [L^2(\Omega)]^d \times L^2(\Omega)$,

$$\begin{aligned} a(\sigma_h-\sigma,\tau) + b_{1,h}(\tau, v_h-u) = a(\sigma_h,\tau)+b_{1,h}(\tau,v_h) &= \sum_{T\in\mathcal{T}_h}\int_T (k_T\nabla v_h + \sigma_h)\cdot\tau \\ &\le \sum_{T\in\mathcal{T}_h} \|\nabla v_h + k_T^{-1}\sigma_h\|_{k;0,T}\ \|\tau\|_{k;0,T}, \end{aligned}$$

and

$$b_2(\sigma_h-\sigma, v) = b_2(\sigma_h, v) - (f,v)_{0,\Omega} = \sum_{T\in\mathcal{T}_h}\int_T (\nabla\cdot\sigma_h - f)\, v \le \sum_{T\in\mathcal{T}_h}\|\nabla\cdot\sigma_h - f\|_{k^{-1};0,T}\ \|v\|_{k;0,T}.$$

Owing to Proposition 2.2 and Remark 2.3, and using the fact that $(\sigma-\sigma_h, u-v_h)\in V$ yields

$$c\varrho_\Omega(k)^{-\frac{1}{2}}(|u-v_h|_{k;1,h} + \|\sigma-\sigma_h\|_{k^{-1};\mathrm{div},\Omega}) \le \sup_{(\tau,v)\in W} \frac{B((\sigma-\sigma_h, u-v_h),(\tau,v))}{\|\tau\|_{k;0,\Omega} + \|v\|_{k;0,\Omega}}.$$

The above estimates, together with the fact that $\nabla\cdot\sigma_h = f_h$ and the triangle inequality, lead to

$$\begin{aligned} c\varrho_\Omega(k)^{-\frac{1}{2}}(|u-v_h|_{k;1,h} + \|\sigma-\sigma_h\|_{k^{-1};\mathrm{div},\Omega}) &\le \left(\sum_{T\in\mathcal{T}_h} \|k_T^{-1}\sigma_h + \nabla v_h\|^2_{k;0,T} + \|f-\nabla\cdot\sigma_h\|^2_{k^{-1};0,T}\right)^{\frac{1}{2}} \\ &\le 2^{\frac{1}{2}}\left(|u_h - v_h|^2_{k;1,h} + \|f-f_h\|^2_{k^{-1};0,\Omega} + \sum_{T\in\mathcal{T}_h}\|k_T^{-1}\sigma_h + \nabla u_h\|^2_{k;0,T}\right)^{\frac{1}{2}}. \end{aligned}$$

Using again the triangle inequality and the fact that $\varrho_\Omega(k)\ge 1$ yields

$$|u-u_h|_{k;1,h} + \|\sigma-\sigma_h\|_{k^{-1};\mathrm{div},\Omega} \le c'\varrho_\Omega(k)^{\frac{1}{2}}\left(|u_h - v_h|^2_{k;1,h} + \|f-f_h\|^2_{k^{-1};0,\Omega} + \sum_{T\in\mathcal{T}_h}\|k_T^{-1}\sigma_h + \nabla u_h\|^2_{k;0,T}\right)^{\frac{1}{2}},$$

with $c' = 1 + \frac{2^{\frac{1}{2}}}{c}$. Finally, use the reconstruction formula (2.8) to infer (3.5). □

Remark 3.3. The *a posteriori* error estimator in (3.5) is the sum of a pre-processing term only depending on f and the mesh plus a post-processing term also depending on the discrete pressure u_h.

The following result is a direct consequence of (3.4), (3.5), and the shape-regularity of the mesh family $(\mathcal{T}_h)_h$.

Corollary 3.4. *Let* (σ, u) *and* (σ_h, u_h) *be respectively the unique solution of* (1.3) *and* (2.4). *Then, under Hypothesis* 3.1*, there exists a constant c such that*

$$|u-u_h|_{k;1,h} + \|\sigma-\sigma_h\|_{k^{-1};\mathrm{div},\Omega} \le c\varrho_\Omega(k)^{\frac{1}{2}} \left(\sum_{T\in\mathcal{T}_h} \mathcal{P}_{1,T}(f)^2 + \sum_{T\in\mathcal{T}_h} \eta_{1,T}(u_h)^2 \right)^{\frac{1}{2}} \tag{3.7}$$

$$\le c\varrho_\Omega(k)^{\frac{1}{2}} \left(\sum_{T\in\mathcal{T}_h} \mathcal{P}_{1,T}(f)^2 + \sum_{F\in\mathcal{F}_h} \eta_{2,F}(u_h)^2 \right)^{\frac{1}{2}}, \tag{3.8}$$

where we have introduced the local error indicators

$$\forall T \in \mathcal{T}_h, \quad \eta_{1,T}(u_h) = |u_h - \mathcal{I}_{\mathrm{Os}} u_h|_{k;1,T}, \tag{3.9}$$

$$\forall F \in \mathcal{F}_h, \quad \eta_{2,F}(u_h) = \{k\}_F^{\frac{1}{2}} h_F^{-\frac{1}{2}} \|[u_h]_F\|_{0,F}. \tag{3.10}$$

Remark 3.5. Both estimators in (3.7) and (3.8) are accessible to computation. The costs for evaluating each are roughly equivalent; see Section 5 for further discussion.

Finally, we investigate the optimality of the above error indicators.

Proposition 3.6. *Let* (σ, u) *and* (σ_h, u_h) *be respectively the unique solution of* (1.3) *and* (2.4). *Then, there exists a constant c such that*

$$\forall T \in \mathcal{T}_h, \quad \mathcal{P}_{1,T}(f) \le \|\sigma - \sigma_h\|_{k^{-1};\mathrm{div},T} + |u-u_h|_{k;1,T}, \tag{3.11}$$

$$\forall F \in \mathcal{F}_h, \quad \eta_{2,F}(u_h) \le c\, \varrho_F(k)^{\frac{1}{2}} \sum_{T'\in\mathcal{T}_F} |u-u_h|_{k;1,T'}, \tag{3.12}$$

$$\forall T \in \mathcal{T}_h, \quad \eta_{1,T}(u_h) \le c \sum_{F\in\mathcal{F}_T^{\mathrm{Os}}} \varrho_F(k)^{\frac{1}{2}} \sum_{T'\in\mathcal{T}_F} |u-u_h|_{k;1,T'}. \tag{3.13}$$

Proof. The local reconstruction formula (2.8) as well as equations (1.3) and (2.9) yield

$$\begin{aligned}\mathcal{P}_{1,T}(f) &= \|\nabla\cdot(\sigma-\sigma_h)\|_{k^{-1};0,T} + \|\sigma_h + k_T \nabla u_h\|_{k^{-1};0,T} \\ &\le \|\sigma-\sigma_h\|_{k^{-1};\mathrm{div},T} + |u-u_h|_{k;1,T}.\end{aligned}$$

Furthermore, there exists a constant c such that

$$\forall v \in H_0^1(\Omega),\ \forall v_h \in P^1_{\mathrm{nc},0}(\mathcal{T}_h),\ \forall F \in \mathcal{F}_h, \quad h_F^{-\frac{1}{2}} \|[v_h]\|_{0,F} \le c \sum_{T\in\mathcal{T}_F} |v-v_h|_{1,T}. \tag{3.14}$$

Estimate (3.14) is established in ([4], Th. 10) for $F \in \mathcal{F}_h^i$, and the proof for $F \in \mathcal{F}_h^\partial$ is similar. Using (3.14), (3.12) is readily deduced. Finally, (3.13) results from (3.4) and (3.12).

□

3.3. Estimators based on the primal formulation

In this section we first derive an *a posteriori* error estimator for the pressure based on the primal formulation and then deduce an *a posteriori* error estimator for the velocity. The analysis relies on Hypothesis 3.1 which in three dimensions must be completed by the following hypothesis (in two dimensions, this hypothesis directly results from Hypothesis 3.1).

Hypothesis 3.7. *All the elements in $\mathcal{T}_h$ having a vertex on the boundary can be connected to an element having a boundary face along a path of adjacent elements containing this vertex and on which the function k is non-decreasing.*

Proposition 3.8. *Let u and u_h be respectively the unique solution of* (1.4) *and* (2.6). *Then, under Hypotheses* 3.1 *and* 3.7*, there exists a constant c such that*

$$|u-u_h|_{k;1,h} \leq c\left(\sum_{T\in\mathcal{T}_h} \mathcal{P}_{2,T}(f)^2 + \inf_{v_h\in P^1_{c,0}(\mathcal{T}_h)} |u_h-v_h|^2_{k;1,h}\right)^{\frac{1}{2}}, \tag{3.15}$$

where we have introduced the local error indicators

$$\forall T\in\mathcal{T}_h,\quad \mathcal{P}_{2,T}(f) = h_T\|f-f_h\|_{k^{-1};0,T} + h_T\|f_h\|_{k^{-1};0,T} + \sum_{F\in\mathcal{F}_T\cap\mathcal{F}_h^i} h_F^{\frac{1}{2}}(k_F^\star)^{-\frac{1}{2}}\|[f_h\pi_h^1\cdot n_F]_F\|_{0,F}. \tag{3.16}$$

Proof. For all $w_h\in P^1_{c,0}(\mathcal{T}_h)$,

$$\Lambda_h(u-u_h,w_h) = (f-f_h,w_h)_{0,\Omega},$$

and therefore, for all $w\in H^1_0(\Omega)$,

$$\Lambda_h(u-u_h,w) = \Lambda_h(u-u_h,w-w_h) + (f-f_h,w_h)_{0,\Omega}.$$

Take $w_h=\mathcal{I}_{\mathrm{BV}}w$. Classical techniques for residual a posteriori estimates [12,32] yield

$$\Lambda_h(u-u_h,w-w_h) \leq c|w|_{k;1,h}\left(\sum_{T\in\mathcal{T}_h}\left(h_T^2\|f_h\|^2_{k^{-1};0,T} + h_T^2\|f-f_h\|^2_{k^{-1};0,T} + \sum_{F\in\mathcal{F}_T\cap\mathcal{F}_h^i} h_F\,(k_F^\star)^{-1}\|[k\nabla u_h\cdot n_F]_F\|^2_{0,F}\right)\right)^{\frac{1}{2}}.$$

Owing to (2.8) and the fact that $\forall F\in\mathcal{F}_h^i$, $[\sigma_h\cdot n_F]_F=0$ since $\sigma_h\in RT^0(\mathcal{T}_h)$, $[k\nabla u_h\cdot n_F]_F=\frac{1}{d}[f_h\pi_h^1\cdot n_F]_F$. Furthermore, to estimate $(f-f_h,w_h)_{0,\Omega}$, use the H^1-stability of $\mathcal{I}_{\mathrm{BV}}$ established in Lemma 3.10 below. This yields

$$\begin{aligned}(f-f_h,w_h)_{0,\Omega} &= (f-f_h,w_h-\Pi^0 w_h)_{0,\Omega} \leq c\sum_{T\in\mathcal{T}_h} h_T\,\|f-f_h\|_{k^{-1};0,T}\,\|\nabla w_h\|_{k;0,T}\\ &\leq c\sum_{T\in\mathcal{T}_h} h_T\,\|f-f_h\|_{k^{-1};0,T}\,\|\nabla w\|_{k;0,\Delta_T} \leq c\left(\sum_{T\in\mathcal{T}_h} h_T^2\,\|f-f_h\|^2_{k^{-1};0,T}\right)^{\frac{1}{2}}|w|_{k;1,h}.\end{aligned}$$

Therefore,

$$\Lambda_h(u-u_h,w) \leq c\left(\sum_{T\in\mathcal{T}_h}\mathcal{P}_{2,T}(f)^2\right)^{\frac{1}{2}}|w|_{k;1,h}.$$

Let v_h be an arbitrary function in $P^1_{c,0}(\mathcal{T}_h)$. Setting $w = u - v_h$ yields $|u - v_h|^2_{k;1,h} = \Lambda_h(u - u_h, w) + \Lambda_h(u_h - v_h, w)$, and hence,

$$|u - v_h|_{k;1,h} \le c \left(\sum_{T\in\mathcal{T}_h} \mathcal{P}_{2,T}(f)^2 + |u_h - v_h|^2_{k;1,h} \right)^{\frac{1}{2}}.$$

Finally, the triangle inequality $|u - u_h|_{k;1,h} \le |u - v_h|_{k;1,h} + |u_h - v_h|_{k;1,h}$ yields the desired estimate. □

Corollary 3.9. *Let u and u_h be respectively the unique solution of* (1.4) *and* (2.6)*. Then, under Hypotheses* 3.1 *and* 3.7*, there exists a constant c such that*

$$|u - u_h|_{k;1,h} \le c \left(\sum_{T\in\mathcal{T}_h} \mathcal{P}_{2,T}(f)^2 + \sum_{T\in\mathcal{T}_h} \eta_{1,T}(u_h)^2 \right)^{\frac{1}{2}} \le c \left(\sum_{T\in\mathcal{T}_h} \mathcal{P}_{2,T}(f)^2 + \sum_{F\in\mathcal{F}_h} \eta_{2,F}(u_h)^2 \right)^{\frac{1}{2}}. \quad (3.17)$$

Lemma 3.10. *Under Hypotheses* 3.1 *and* 3.7*, there exists a constant c such that*

$$\forall v \in H^1_0(\Omega),\ \forall T \in \mathcal{T}_h, \quad |\mathcal{I}_{\mathrm{BV}} v|_{k;1,T} \le c\,|v|_{k;1,\Delta_T}. \quad (3.18)$$

Proof. For a measurable set ω and a function $v \in L^1(\omega)$, denote by $\mu_\omega(v)$ the mean-value of v over ω.

(1) Let us first prove that

$$\forall v \in H^1_0(\Omega),\ \forall F \in \mathcal{F}^i_h,\ F = T_1 \cap T_2, \quad \|\mu_{T_1}(v) - \mu_{T_2}(v)\|_{0,T_1\cup T_2} \le c h_F \|\nabla v\|_{0,T_1\cup T_2}. \quad (3.19)$$

Set $\delta_1 = v - \mu_{T_1}(v)$, $\delta_2 = v - \mu_{T_2}(v)$, and $\delta_{12} = v - \mu_{T_1\cup T_2}(v)$. Owing to the Poincaré–Wirtinger inequality applied on T_1, T_2, and $T_1 \cup T_2$ and a scaling argument, it is readily inferred that

$$\|\delta_1\|_{0,T_1} + \|\delta_2\|_{0,T_2} + \|\delta_{12}\|_{0,T_1\cup T_2} \le c(h_{T_1} + h_{T_2})\|\nabla v\|_{0,T_1\cup T_2}. \quad (3.20)$$

Furthermore,

$$\delta_{12} = \delta_1 + \frac{|T_2|}{|T_1| + |T_2|}(\mu_{T_1}(v) - \mu_{T_2}(v)) = \delta_2 + \frac{|T_1|}{|T_1| + |T_2|}(\mu_{T_2}(v) - \mu_{T_1}(v)).$$

In particular, this yields $|\mu_{T_1}(v) - \mu_{T_2}(v)| \le c(|\delta_{12}| + |\delta_1|)$ on T_1, and $|\mu_{T_1}(v) - \mu_{T_2}(v)| \le c(|\delta_{12}| + |\delta_2|)$ on T_2. The estimate (3.19) then results from (3.20) and the shape-regularity of the mesh family.

(2) For a vertex $s \in \mathcal{V}^i_h$, let ω_s be the support of the nodal basis function φ_s, *i.e.*, the union of all elements in $\mathcal{T}_h$ that have s as a vertex. Let $l(s) \in \{1, \dots, L\}$ be an integer such that s is contained in $\overline{\Omega}_{l(s)}$ and that $k|_{\Omega_{l(s)}}$ is maximal among all $k|_{\Omega_j}$ such that $\overline{\Omega}_j$ contains s. Then, the operator $\mathcal{I}_{\mathrm{BV}}$ is defined as follows:

$$\forall v \in L^2(\Omega), \quad \mathcal{I}_{\mathrm{BV}} v = \sum_{s\in\mathcal{V}^i_h} \mu_{\omega_s\cap\Omega_{l(s)}}(v)\,\varphi_s.$$

(3) Let $T \in \mathcal{T}_h$ and assume first that all the vertices of T are in $\mathcal{V}^i_h$. Then,

$$\nabla\mathcal{I}_{\mathrm{BV}} v|_T = \sum_{s\in T\cap\mathcal{V}^i_h} \mu_{\omega_s\cap\Omega_{l(s)}}(v)\nabla\varphi_s|_T = \sum_{s\in T\cap\mathcal{V}^i_h} (\mu_{\omega_s\cap\Omega_{l(s)}}(v) - \mu_T(v))\nabla\varphi_s|_T. \quad (3.21)$$

Denote by $T_1, \dots, T_{k(s)}$ the triangles in $\omega_s \cap \Omega_{l(s)}$. Then,

$$\mu_{\omega_s\cap\Omega_{l(s)}}(v) - \mu_T(v) = \frac{1}{|T_1| + \ldots + |T_{k(s)}|} \left(\sum_{i=1}^{k(s)} |T_i|(\mu_{T_i}(v) - \mu_T(v)) \right).$$

Owing to the shape-regularity of the mesh family,

$$|\mu_{\omega_s\cap\Omega_{l(s)}}(v)-\mu_T(v)|\le c\sum_{T_1,T_2}|\mu_{T_1}(v)-\mu_{T_2}(v)|,$$

where $\sum_{T_1,T_2}$ denotes a finite sum over triangle pairs that share a face. Moreover, owing to Hypothesis 3.1 and the choice for $\Omega_{l(s)}$, the pairs can always be chosen such that $k_{T_1}\ge k_T$ and $k_{T_2}\ge k_T$. Hence, using (3.19) yields

$$k_T^{\frac{1}{2}}|\mu_{\omega_s\cap\Omega_{l(s)}}(v)-\mu_T(v)|\le ch_T|\omega_s|^{-\frac{1}{2}}|v|_{k;1,\omega_s}. \tag{3.22}$$

Finally, (3.21) and (3.22) imply

$$|\mathcal{I}_{\rm BV}v|_{k;1,T}\le ch_T|\omega_s|^{-\frac{1}{2}}|v|_{k;1,\omega_s}\left(\sum_{s\in T\cap\mathcal{V}_h^i}\|\nabla\varphi_s\|_{0,T}\right)\le c|v|_{k;1,\omega_s}\le c|v|_{k;1,\Delta_T},$$

since $\omega_s\subset\Delta_T$.

(4) Finally, if the vertex s of T lies on the boundary, (3.22) also holds with $\mu_{\omega_s\cap\Omega_{l(s)}}(v)=0$. Indeed, firstly assume that T has a face lying on the boundary. Then, one can proceed as in step 1 by extending v by zero outside Ω to prove that $\|\mu_T(v)\|_{0,T}\le ch_T\|\nabla v\|_{0,T}$, yielding (3.22). If T has less than a face lying on the boundary, Hypothesis 3.7 allows to consider a path leading to a triangle with a boundary face along which the function k is non-decreasing. This yields again (3.22) with $\mu_{\omega_s\cap\Omega_{l(s)}}(v)=0$. The conclusion of the proof is then straightforward by replacing in (3.21) the quantity $\mu_{\omega_s\cap\Omega_{l(s)}}(v)$ by 0 for all the vertices of T that lie on the boundary. □

We next investigate the optimality of the above error indicators. Owing to Proposition 3.6, we only need to prove the optimality of $\mathcal{P}_{2,T}(f)$.

Proposition 3.11. *Let u and u_h be respectively the unique solution of* (1.4) *and* (2.6)*. Then, there exists a constant c such that*

$$\forall T\in\mathcal{T}_h,\quad \mathcal{P}_{2,T}(f)\le c(|u-u_h|_{k;1,\Delta_T}+h_T\|f-f_h\|_{k^{-1};0,\Delta_T}). \tag{3.23}$$

Proof. Classical techniques (see, *e.g.*, [12,32]) show that for all $T\in\mathcal{T}_h$,

$$\begin{aligned}\sum_{F\in\mathcal{F}_T}h_F^{\frac{1}{2}}(k_F^\star)^{-\frac{1}{2}}\|[k\nabla u_h\cdot n_F]_F\|_{0,F}&\le c\sum_{F\in\mathcal{F}_T}\sum_{T'\in\mathcal{T}_F}\left(|u-u_h|_{k;1,T'}+h_T\|f-f_h\|_{k^{-1};0,T'}\right)\\&\le c\left(|u-u_h|_{k;1,\Delta_T}+h_T\|f-f_h\|_{k^{-1};0,\Delta_T}\right),\end{aligned}$$

and $h_T\|f_h\|_{k^{-1};0,T}\le c\left(|u-u_h|_{k;1,T}+h_T\|f-f_h\|_{k^{-1};0,T}\right)$. The proof is complete. □

Remark 3.12. If $f\in H^1(\mathcal{T}_h)$, $h_T\|f-f_h\|_{k^{-1};0,T}$ is one order higher than $|u-u_h|_{k;1,T}$.

One of the attractive features of the finite volume box scheme (2.4) is that velocity error estimates can be readily deduced from pressure error estimates.

Proposition 3.13. *Let (σ,u) and (σ_h,u_h) be respectively the unique solution of* (1.3) *and* (2.4)*. Assume that there exists a pressure error indicator $\eta_T(\mathcal{T}_h,f,u_h)$ depending on the mesh $\mathcal{T}_h$, the data f, and the discrete pressure u_h such that*

$$|u-u_h|_{k;1,h}\le\chi^*\left(\sum_{T\in\mathcal{T}_h}\eta_T(\mathcal{T}_h,f,u_h)^2\right)^{\frac{1}{2}}, \tag{3.24}$$

and

$$\forall T \in \mathcal{T}_h, \quad \chi_* \, \eta_T(\mathcal{T}_h, f, u_h) \le |u - u_h|_{k;1,\Delta_T}, \tag{3.25}$$

for some constants χ_* *and* χ^*. *Then,*

$$\|\sigma - \sigma_h\|_{k^{-1};\mathrm{div},\Omega} \le 2 \left((\chi^*)^2 \sum_{T\in\mathcal{T}_h} \eta_T(\mathcal{T}_h, f, u_h)^2 + \sum_{T\in\mathcal{T}_h} \mathcal{P}_{1,T}(f)^2 \right)^{\frac{1}{2}}, \tag{3.26}$$

and

$$\chi_* \eta_T(\mathcal{T}_h, f, u_h) + \mathcal{P}_{1,T}(f) \le 3|u - u_h|_{k;1,\Delta_T} + 2\|\sigma - \sigma_h\|_{k^{-1};\mathrm{div},T}. \tag{3.27}$$

Proof. The local reconstruction formula (2.8) yields

$$\|\sigma - \sigma_h\|^2_{k^{-1};0,\Omega} \le 2 \sum_{T\in\mathcal{T}_h} \left(|u - u_h|^2_{k;1,T} + \frac{1}{d^2}\rho_T^2 \|f_h\|^2_{k^{-1};0,T} \right).$$

Since $\nabla\cdot(\sigma - \sigma_h) = f - f_h$, this yields

$$\|\nabla\cdot(\sigma - \sigma_h)\|^2_{k^{-1};0,\Omega} + \|\sigma - \sigma_h\|^2_{k^{-1};0,\Omega} \le 2 \left((\chi^*)^2 \sum_{T\in\mathcal{T}_h} \eta_T(\mathcal{T}_h, f, u_h)^2 + \sum_{T\in\mathcal{T}_h} \mathcal{P}_{1,T}(f)^2 \right),$$

yielding estimate (3.26). To prove (3.27), first notice that

$$\mathcal{P}_{1,T}(f)^2 \le 2 \left(\|\nabla\cdot(\sigma - \sigma_h)\|^2_{k^{-1};0,T} + \frac{1}{d^2}\rho_T^2 \|f_h\|^2_{k^{-1};0,T} \right),$$

and owing to the local reconstruction formula (2.8),

$$\frac{1}{d^2}\rho_T^2 \|f_h\|^2_{k^{-1};0,T} \le 2 \left(\|\sigma - \sigma_h\|^2_{k^{-1};0,T} + \|\nabla(u - u_h)\|^2_{k;0,T} \right).$$

Therefore,

$$\mathcal{P}_{1,T}(f)^2 \le 4 \left(\|\sigma - \sigma_h\|^2_{k^{-1};\mathrm{div},T} + |u - u_h|^2_{k;1,T} \right),$$

whence (3.27) is easily deduced. □

4. Hierarchical *a posteriori* error analysis

In this section we derive hierarchical *a posteriori* error estimates in the framework of the primal formulation (2.6). *A posteriori* error estimates for the velocity can then be easily deduced from Proposition 3.13. Firstly, we establish global upper bounds and local lower bounds for the pressure error using classical techniques relying on a saturation assumption and a strengthened Cauchy–Schwarz inequality [2, 8]. Secondly, extending the techniques presented in [1] for conforming settings to nonconforming settings, we circumvent the need for the saturation assumption.

To enrich the space $P^1_{\mathrm{nc},0}(\mathcal{T}_h)$ we make the following assumption:

Hypothesis 4.1. *There exists a space* $\widehat{X}_h \subset H^1(\mathcal{T}_h)$ *such that:*

(i) $P^1_{\mathrm{nc},0}(\mathcal{T}_h)$ *and* $\widehat{X}_h$ *form a direct sum, henceforth denoted by* $\overline{X}_h$;

(ii) $\forall \widehat{x}_h \in \widehat{X}_h$, $\forall F \in \mathcal{F}_h$, $\int_F [\widehat{x}_h]_F = 0$.

Consider the two following problems:

$$\begin{cases} \text{Find } \overline{u}_h \in \overline{X}_h \text{ such that} \\ \Lambda_h(\overline{u}_h, \overline{v}_h) = (f_h, \overline{v}_h)_{0,\Omega} \quad \forall \overline{v}_h \in \overline{X}_h, \end{cases} \tag{4.1}$$

and

$$\begin{cases} \text{Find } \widehat{u}_h \in \widehat{X}_h \text{ such that} \\ \Lambda_h(\widehat{u}_h, \widehat{v}_h) = (f_h, \widehat{v}_h)_{0,\Omega} - \Lambda_h(u_h, \widehat{v}_h) \quad \forall \widehat{v}_h \in \widehat{X}_h, \end{cases} \tag{4.2}$$

where u_h is the unique solution of the primal formulation (2.6). Owing to Hypothesis 4.1(ii), $|\cdot|_{k;1,h}$ is a norm on $\overline{X}_h$. Hence, problems (4.1) and (4.2) admit a unique solution.

4.1. Hierarchical estimators relying on a saturation assumption

Two hierarchical *a posteriori* error estimators are derived in this section, one based on conforming face bubbles and one based on nonconforming element bubbles. Both estimators rely on the following hypotheses:

Hypothesis 4.2 (saturation assumption)**.** *There exists a constant* $\beta \in (0,1)$ *independent of* h *and of* $\varrho_\Omega(k)$ *such that*

$$|u - \overline{u}_h|_{k;1,h} \leq \beta\, |u - u_h|_{k;1,h}. \tag{4.3}$$

Hypothesis 4.3. *There exists a constant* $\gamma \in [0,1)$ *independent of* h *such that*

$$\forall v_h \in P^1_{\mathrm{nc},0}(\mathcal{T}_h),\ \forall w_h \in \widehat{X}_h,\ \forall T \in \mathcal{T}_h, \quad (\nabla v_h, \nabla w_h)_{0,T} \leq \gamma |v_h|_{1,T} |w_h|_{1,T}. \tag{4.4}$$

Clearly, Hypothesis 4.3 implies the strengthened Cauchy–Schwarz inequality

$$\forall v_h \in P^1_{\mathrm{nc},0}(\mathcal{T}_h),\ \forall w_h \in \widehat{X}_h, \quad \Lambda_h(v_h, w_h) \leq \gamma |v_h|_{k;1,h} |w_h|_{k;1,h}. \tag{4.5}$$

Proposition 4.4. *Let* u *and* u_h *be respectively the unique solution of* (1.4) *and* (2.6)*. Then, under Hypotheses* 4.1*,* 4.2*, and* 4.3*, the following holds:*

$$|u - u_h|_{k;1,h} \leq (1-\beta)^{-1}(1-\gamma^2)^{-\frac{1}{2}} |\widehat{u}_h|_{k;1,h}. \tag{4.6}$$

Proof. The proof is a straightforward extension to the nonconforming case of the ideas presented in [8]. Let $\overline{u}_h$ solve (4.1). Set $\overline{u}_h = u_1 + u_2$ where $u_1 \in P^1_{\mathrm{nc},0}(\mathcal{T}_h)$ and $u_2 \in \widehat{X}_h$. For $v_h \in P^1_{\mathrm{nc},0}(\mathcal{T}_h) \subset \overline{X}_h$,

$$\Lambda_h(\overline{u}_h - u_h, v_h) = 0,$$

and for all $\widehat{v}_h \in \widehat{X}_h \subset \overline{X}_h$,

$$\Lambda_h(\overline{u}_h - u_h, \widehat{v}_h) = \Lambda_h(\widehat{u}_h, \widehat{v}_h)\,.$$

Thus, taking $v_h = u_1 - u_h$ and $\widehat{v}_h = u_2$ in the above equations yields

$$|\overline{u}_h - u_h|^2_{k;1,h} = \Lambda_h(\widehat{u}_h, u_2),$$

and owing to the (standard) Cauchy–Schwarz inequality, $|\overline{u}_h - u_h|^2_{k;1,h} \leq |\widehat{u}_h|_{k;1,h} |u_2|_{k;1,h}$. Furthermore, owing to (4.5),

$$|u_1 - u_h|^2_{k;1,h} + |u_2|^2_{k;1,h} - |\overline{u}_h - u_h|^2_{k;1,h} = 2\Lambda_h(u_2, u_h - u_1) \leq 2\gamma |u_2|_{k;1,h} |u_h - u_1|_{k;1,h}.$$

Therefore, $(1-\gamma^2)|u_2|^2_{k;1,h} \le |\overline{u}_h - u_h|^2_{k;1,h}$, implying $|u_h - \overline{u}_h|_{k;1,h} \le (1-\gamma^2)^{-\frac{1}{2}} |\widehat{u}_h|_{k;1,h}$. Combining the above inequalities and using the triangle inequality leads to

$$|u - u_h|_{k;1,h} \le |u - \overline{u}_h|_{k;1,h} + (1-\gamma^2)^{-\frac{1}{2}} |\widehat{u}_h|_{k;1,h}.$$

Conclude using Hypothesis 4.2. □

4.1.1. *Hierarchical estimator using conforming face bubbles*

Let $T \in \mathcal{T}_h$ and number its faces as $\{F_i\}_{0\le i\le d}$. For $0 \le i \le d$, let $\lambda_{i,T}$ be the barycentric coordinate associated with the vertex of T opposite to F_i. Let T'_i be the simplex whose vertices are the barycenter of T and the d vertices of F_i.

For $F \in \mathcal{F}_h^i$, $F = T_1 \cap T_2$, denote by i_1 and i_2 the local index of F in T_1 and T_2, respectively. Set $\widetilde{\Delta}_F = T'_{i_1} \cup T'_{i_2}$ and introduce the conforming face bubble $b_F^{\rm c}$ defined as follows:

$$\begin{cases} b_F^{\rm c}|_{T'_{i_m}} = d^d \displaystyle\prod_{\substack{j=0 \\ j\ne i_m}}^{j=d} (\lambda_{j,T_m} - \lambda_{i_m,T_m}), \quad m = 1, 2, \\ b_F^{\rm c}|_{\Omega\setminus\widetilde{\Delta}_F} = 0. \end{cases} \tag{4.7}$$

Finally, set

$$\widehat{X}_h = \mathcal{B}_{\rm c}(\mathcal{T}_h) = \mathrm{span}_{F\in\mathcal{F}_h^i} \{b_F^{\rm c}\}. \tag{4.8}$$

It is clear that Hypothesis 4.1 holds.

Proposition 4.5. *Let u and u_h be respectively the unique solution of* (1.4) *and* (2.6)*. Then, under Hypotheses* 4.2 *and* 4.3*, there exists a constant c such that*

$$|u - u_h|_{k;1,h} \le c \left(\sum_{F\in\mathcal{F}_h^i} \mathcal{P}_{3,F}(f)^2 \right)^{\frac{1}{2}}, \tag{4.9}$$

where we have introduced the local error indicators

$$\forall F \in \mathcal{F}_h^i, \quad \mathcal{P}_{3,F}(f) = \frac{|(f_h, b_F^{\rm c})_{0,\widetilde{\Delta}_F} - \frac{1}{d}[f_h \pi_h^1 \cdot n_F]_F \int_F b_F^{\rm c}|}{|b_F^{\rm c}|_{k;1,\widetilde{\Delta}_F}}. \tag{4.10}$$

Proof. Let us show that

$$\forall F \in \mathcal{F}_h^i, \quad |\widehat{u}_h|_{k;1,\widetilde{\Delta}_F} = \mathcal{P}_{3,F}(f), \tag{4.11}$$

where $|\widehat{u}_h|_{k;1,\widetilde{\Delta}_F} = \left(\sum_{T'\in\widetilde{\Delta}_F} |\widehat{u}_h|^2_{k;1,T'}\right)^{\frac{1}{2}}$. Take $\widehat{v}_h = b_F^{\rm c}$ in (4.2). An integration by parts and the reconstruction formula (2.8) lead to

$$\begin{aligned} \sum_{T'\in\widetilde{\Delta}_F} (k_T \nabla\widehat{u}_h, \nabla b_F^{\rm c})_{0,T'} &= (f, b_F^{\rm c})_{0,\widetilde{\Delta}_F} - \sum_{T'\in\widetilde{\Delta}_F} (k_T \nabla u_h, \nabla b_F^{\rm c})_{0,T'} \\ &= (f, b_F^{\rm c})_{0,\widetilde{\Delta}_F} - \int_F [k\nabla u_h \cdot n_F]_F b_F^{\rm c} = (f, b_F^{\rm c})_{0,\widetilde{\Delta}_F} - \tfrac{1}{d}[f_h \pi_h^1 \cdot n_F]_F \int_F b_F^{\rm c}. \end{aligned}$$

Set $\widehat{u}_h|_{\widetilde{\Delta}_F} = \alpha_F b_F^{\rm c}$ with $\alpha_F \in \mathbb{R}$. Then, $\sum_{T'\in\widetilde{\Delta}_F} (k_T \nabla\widehat{u}_h, \nabla b_F^{\rm c})_{0,T'} = \alpha_F |b_F^{\rm c}|^2_{k;1,\widetilde{\Delta}_F}$, yielding

$$\alpha_F = \frac{(f_h, b_F^{\rm c})_{0,\widetilde{\Delta}_F} - \frac{1}{d}[f_h \pi_h^1 \cdot n_F]_F \int_F b_F^{\rm c}}{|b_F^{\rm c}|^2_{k;1,\widetilde{\Delta}_F}},$$

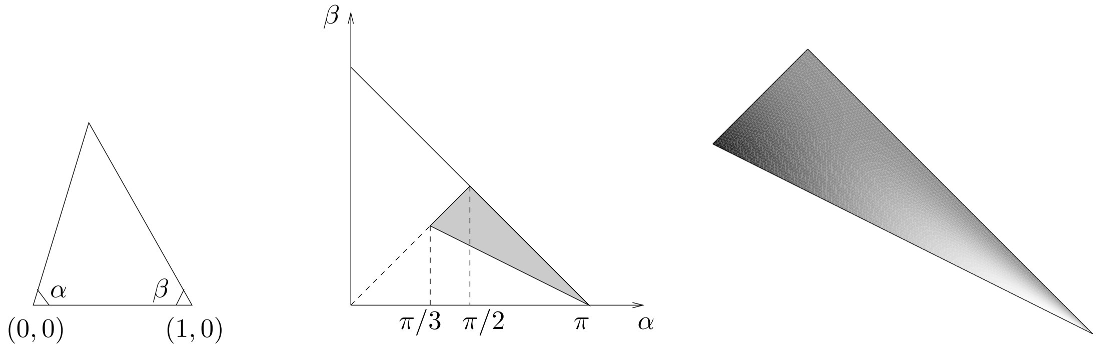

FIGURE 1. Left: triangle T with angles α and β; middle: domain D (shaded triangle) for pairs (α, β); right: function $(\alpha, \beta) \in D \mapsto \gamma_T$ (in the color table, black values correspond to 0.4 and white values to 0.75).

and (4.11) results from the fact that $|\widehat{u}_h|_{k;1,\widetilde{\Delta}_F} = |\alpha_F||b_F^{\mathrm{c}}|_{k;1,\widetilde{\Delta}_F}$. Finally, the estimate (4.9) directly results from (4.6) and (4.11). $\square$

Remark 4.6. The *a posteriori* error indicator (4.10) only involves a pre-processing term.

In the two-dimensional case, it is relatively straightforward to verify the strengthened Cauchy–Schwarz inequality.

Lemma 4.7. *Assume $d = 2$. Then, there exists a constant $\gamma < 1$ such that* (4.4) *is verified.*

Proof. The proof relies on numerical verification of the statement rather than formal mathematical arguments.

(1) For $T \in \mathcal{T}_h$, let $\mathcal{B}_c(T) = \mathrm{span}_{F \subset \partial T}\{b_F^{\mathrm{c}}|_T\}$ and let

$$\gamma_T = \max_{u \in P^1(T), v \in \mathcal{B}_c(T)} \frac{(\nabla u, \nabla v)_{0,T}}{\|\nabla u\|_{0,T}\|\nabla v\|_{0,T}}.$$

It is easily verified that $\gamma_T = \sup_{x \in \mathbb{R}^3} \frac{x^t A_{12} A_{22}^{-1} A_{21} x}{x^t A_{11} x}$, where A_{11}, A_{12}, A_{21}, and A_{22} are the 3×3 blocks of the local stiffness matrix A relative to the basis functions of $P^1_{\mathrm{nc},0}(\mathcal{T}_h)$ and $\mathcal{B}_{\mathrm{c}}(\mathcal{T}_h)$ (see, *e.g.*, [5], p. 97, or [22], p. 441).

(2) Let $T \in \mathcal{T}_h$. Owing to isotropy and scale invariance, we can assume that two of the vertices of the triangle T have coordinates $(0, 0)$ and $(1, 0)$ and parameterize the triangle T by its angles (α, β) (see left plot in Fig. 1). For each (α, β), we solve the above eigenvalue problem numerically and thus construct the function $(\alpha, \beta) \mapsto \gamma_T$. Again, because of isotropy and scale invariance, the same result is obtained for γ_T if any two angles are taken from the set $\{\, \alpha, \beta, \pi - \alpha - \beta \,\}$ in whichever order. Therefore, the investigation can be restricted to the domain

$$D = \{\, (\alpha, \beta);\ \alpha \geq \beta;\ \alpha + 2\beta \geq \pi;\ \alpha + \beta \leq \pi \,\}.$$

This domain is depicted in the middle plot of Figure 1 as a shaded triangle. Isocontours for the function $(\alpha, \beta) \in D \mapsto \gamma_T$ are presented on the right plot in Figure 1. The minimum value for γ_T is 0.4 and is attained for an equilateral triangle (left corner of shaded triangle). The maximum value, 0.75, corresponds to $\alpha \to \pi$. Therefore, it is possible to bound γ_T from above by a constant $\gamma < 1$. $\square$

Finally, we investigate the optimality of the error indicator (4.10).

Proposition 4.8. *Let u and u_h be respectively the unique solution of* (1.4) *and* (2.6). *Then, there exists a constant c such that*

$$\forall F \in \mathcal{F}_h^i, \quad \mathcal{P}_{3,F}(f) \le |u - u_h|_{k;1,\widetilde{\Delta}_F} + c h_F \|f - f_h\|_{k^{-1};0,\widetilde{\Delta}_F}. \tag{4.12}$$

Proof. Since $\widehat{u}_h$ solves (4.2) and $\widehat{X}_h \subset H_0^1(\Omega)$,

$$\begin{aligned} |\widehat{u}_h|^2_{k;1,\widetilde{\Delta}_F} &= \sum_{T' \in \widetilde{\Delta}_F} \int_{T'} k|_{T'} \nabla(u - u_h)\cdot\nabla\widehat{u}_h + \int_{\widetilde{\Delta}_F} (f_h - f)\,\widehat{u}_h \\ &\le |u - u_h|_{k;1,\widetilde{\Delta}_F} |\widehat{u}_h|_{k;1,\widetilde{\Delta}_F} + \|f - f_h\|_{0,\widetilde{\Delta}_F} \|\widehat{u}_h\|_{0,\widetilde{\Delta}_F}. \end{aligned}$$

Since $\|b_F^{\mathrm{c}}\|_{0,\widetilde{\Delta}_F} \le c h_F \|\nabla b_F^{\mathrm{c}}\|_{0,\widetilde{\Delta}_F}$ and $\widehat{u}_h$ is proportional to b_F^{c} on $\widetilde{\Delta}_F$, the desired estimate holds. □

4.1.2. *Hierarchical estimator using nonconforming element bubbles*

Let $T \in \mathcal{T}_h$. Consider the nonconforming element bubble b_T^{nc} introduced by Fortin–Soulié [23] such that

$$\begin{cases} b_T^{\mathrm{nc}}|_T = 2 - (d+1) \sum_{i=0}^{d} \lambda_{i,T}^2, \\ b_T^{\mathrm{nc}}|_{\Omega\setminus T} = 0. \end{cases} \tag{4.13}$$

Note that the nonconforming element bubbles are such that

$$\forall T \in \mathcal{T}_h,\ \forall F \in \mathcal{F}_h, \quad \int_F b_T^{\mathrm{nc}} = 0. \tag{4.14}$$

Indeed, in two dimensions, b_T^{nc} vanishes at the two Gauß points with edge barycentric coordinates $\frac{1}{2} \pm \frac{1}{2}(\frac{1}{3})^{\frac{1}{2}}$ whereas in three dimensions, b_T^{nc} vanishes at the three Gauß points with face barycentric coordinates $(\frac{2}{3}, \frac{1}{6}, \frac{1}{6})$. Finally, set

$$\widehat{X}_h = \mathcal{B}_{\mathrm{nc}}(\mathcal{T}_h) = \mathrm{span}_{T \in \mathcal{T}_h} \{b_T^{\mathrm{nc}}\}. \tag{4.15}$$

It is clear that Hypothesis 4.1 holds.

Lemma 4.9.

(i) The strengthened Cauchy–Schwarz inequality holds for spaces $P^1_{\mathrm{nc},0}(\mathcal{T}_h)$ and $\mathcal{B}_{\mathrm{nc}}(\mathcal{T}_h)$ with $\gamma = 0$.

(ii) Let $\overline{u}_h = u_1 + u_2$ be the unique decomposition of the solution $\overline{u}_h$ of (4.1) *with $u_1 \in P^1_{\mathrm{nc},0}(\mathcal{T}_h)$ and $u_2 \in \mathcal{B}_{\mathrm{nc}}(\mathcal{T}_h)$. Then $u_1 = u_h$ is the unique solution of* (2.6) *and $u_2 = \widehat{u}_h$ is the unique solution of* (4.2).

Proof.

(i) Let v_b be an arbitrary function in $\mathcal{B}_{\mathrm{nc}}(\mathcal{T}_h)$ and let v_h be an arbitrary function in $P^1_{\mathrm{nc},0}(\mathcal{T}_h)$. Let $T \in \mathcal{T}_h$. The Green formula yields

$$(\nabla v_b, \nabla v_h)_{0,T} = \sum_{F \in \mathcal{F}_T} \nabla v_h \cdot n_F \int_F v_b,$$

and the right-hand side vanishes owing to (4.14). This implies that the strengthened Cauchy–Schwarz inequality holds for spaces $P^1_{\mathrm{nc},0}(\mathcal{T}_h)$ and $\mathcal{B}_{\mathrm{nc}}(\mathcal{T}_h)$ with $\gamma = 0$.

(ii) Let $\overline{u}_h = u_1 + u_2$ be the unique decomposition of the solution $\overline{u}_h$ of (4.1) with $u_1 \in P^1_{\mathrm{nc},0}(\mathcal{T}_h)$ and $u_2 \in \mathcal{B}_{\mathrm{nc}}(\mathcal{T}_h)$. For all $v_h \in P^1_{\mathrm{nc},0}(\mathcal{T}_h)$,

$$(f_h, v_h)_{0,\Omega} = \Lambda_h(\overline{u}_h, v_h) = \Lambda_h(u_1, v_h) + \Lambda_h(u_2, v_h),$$

and owing to the first part of the proof, $\Lambda_h(u_2, v_h) = 0$. Hence, $\Lambda_h(u_1, v_h) = (f_h, v_h)_{0,\Omega}$, *i.e.*, u_1 is the unique solution of (2.6), and this in turn implies that u_2 is the unique solution of (4.2). □

Proposition 4.10. *Let u and u_h be respectively the unique solution of* (1.4) *and* (2.6). *Then, under Hypothesis* 4.3,

$$\frac{1}{1+\beta}\left(\sum_{T\in\mathcal{T}_h} \mathcal{P}_{4,T}(f)^2\right)^{\frac{1}{2}} \le |u-u_h|_{k;1,h} \le \frac{1}{1-\beta}\left(\sum_{T\in\mathcal{T}_h} \mathcal{P}_{4,T}(f)^2\right)^{\frac{1}{2}}, \tag{4.16}$$

where we have introduced the local error indicators

$$\forall T\in\mathcal{T}_h, \quad \mathcal{P}_{4,T}(f) = \frac{(f_h, b_T^{\mathrm{nc}})_{0,T}}{|b_T^{\mathrm{nc}}|_{k;1,T}}. \tag{4.17}$$

Proof.

(1) Let $\overline{u}_h$ be the unique solution of (4.1). Using Lemma 4.9, set $\overline{u}_h = u_h + \widehat{u}_h$. Therefore,

$$|\widehat{u}_h|_{k;1,h} = |\overline{u}_h - u_h|_{k;1,h} \le |u-\overline{u}_h|_{k;1,h} + |u-u_h|_{k;1,h} \le (1+\beta)|u-u_h|_{k;1,h},$$

owing to Hypothesis 4.2. Furthermore, since the constant γ in Hypothesis 4.3 is simply 0, Proposition 4.6 yields $|u-u_h|_{k;1,h} \le \frac{1}{1-\beta}|\widehat{u}_h|_{k;1,h}$. As a result,

$$\frac{1}{1+\beta}|\widehat{u}_h|_{k;1,h} \le |u-u_h|_{k;1,h} \le \frac{1}{1-\beta}|\widehat{u}_h|_{k;1,h}.$$

(2) To conclude the proof, let us show that $|\widehat{u}_h|_{k;1,T} = \mathcal{P}_{4,T}(f)$ for all $T\in\mathcal{T}_h$. Taking $\widehat{v}_h = b_T^{\mathrm{nc}}$ in (4.2) and using the fact that $(\nabla u_h, \nabla b_T^{\mathrm{nc}})_{0,T} = 0$, yields

$$\forall T\in\mathcal{T}_h, \quad k_T(\nabla\widehat{u}_h, \nabla b_T^{\mathrm{nc}})_{0,T} = (f_h, b_T^{\mathrm{nc}})_{0,T}.$$

Set $\widehat{u}_h|_T = \alpha_T b_T^{\mathrm{nc}}$ for some $\alpha_T\in\mathbb{R}$. Since $(\nabla\widehat{u}_h, \nabla b_T^{\mathrm{nc}})_{0,T} = \alpha_T|b_T^{\mathrm{nc}}|_{1,T}^2$, it is inferred that $\alpha_T = \dfrac{(f_h, b_T^{\mathrm{nc}})_{0,T}}{|b_T^{\mathrm{nc}}|_{k;1,T}^2}$, and hence $|\widehat{u}_h|_{k;1,T} = \mathcal{P}_{4,T}(f)$. □

Remark 4.11. Since $\overline{u}_h$ can be computed without solving problem (4.1), it is relatively cheap to verify the saturation assumption numerically.

Remark 4.12. The *a posteriori* error estimator in (4.16) only involves a pre-processing term.

4.2. Hierarchical estimator circumventing the saturation assumption

In this section we analyze a hierarchical *a posteriori* error estimator that circumvents Hypotheses 4.2 and 4.3. We consider the case $\widehat{X}_h = \mathcal{B}_{\mathrm{c}}(\mathcal{T}_h)$.

Proposition 4.13. *Let u and u_h be respectively the unique solution of* (1.4) *and* (2.6). *Then, under Hypotheses* 3.1 *and* 3.7, *there exists a constant c such that*

$$|u-u_h|_{k;1,h} \le c\left(\sum_{F\in\mathcal{F}_h^i} \mathcal{P}_{3,F}(f)^2 + \sum_{T\in\mathcal{T}_h} \mathcal{P}_{5,T}(f)^2 + \inf_{v_h\in P_{c,0}^1(\mathcal{T}_h)} |u_h - v_h|_{k;1,h}^2\right)^{\frac{1}{2}}, \tag{4.18}$$

where we have introduced the local error indicators

$$\forall T \in \mathcal{T}_h, \quad \mathcal{P}_{5,T}(f) = h_T \|f\|_{k^{-1};0,T} + h_T \|f - f_h\|_{k^{-1};0,T}. \tag{4.19}$$

Proof.

(1) Let $\Pi : H_0^1(\Omega) \to \mathcal{B}_{\mathrm{c}}(\mathcal{T}_h)$ be the interpolation operator defined for $v \in H_0^1(\Omega)$ as

$$\Pi v = \sum_{F \in \mathcal{F}_h^i} \left(\frac{\int_F v}{\int_F b_F^{\mathrm{c}}} \right) b_F^{\mathrm{c}}. \tag{4.20}$$

An integration by parts readily shows that $\Lambda_h(v_h, v) = \Lambda_h(v_h, \Pi v)$ for all $v_h \in P^1_{\mathrm{nc},0}(\mathcal{T}_h)$ and $v \in H_0^1(\Omega)$. Furthermore, the operator Π is endowed with the following stability property: There exists a constant c such that for all $v \in H_0^1(\Omega)$ and $T \in \mathcal{T}_h$,

$$\|\Pi v\|_{1,T} \le c h_T^{-\frac{1}{2}} \sum_{F \in \mathcal{F}_T} \|v\|_{0,F}, \tag{4.21}$$

$$\|\Pi v\|_{0,T} \le c h_T^{\frac{1}{2}} \sum_{F \in \mathcal{F}_T} \|v\|_{0,F}. \tag{4.22}$$

Inequality (4.21) is established in ([1], Lem. 2.2). To establish (4.22), first notice that owing to the shape-regularity of $(\mathcal{T}_h)_h$ and to the construction of b_F^{c}, there exists a constant c such that for all $T \in \mathcal{T}_h$ and $F \in \mathcal{F}_T$, $|F|^{\frac{1}{2}} \|b_F^{\mathrm{c}}\|_{0,T} \le c h_T^{\frac{1}{2}} \int_F b_F^{\mathrm{c}}$ where $|F|$ denotes the $(d{-}1)$-measure of F. Using (4.20) and the Cauchy–Schwarz inequality yields

$$\|\Pi v\|_{0,T} \le \sum_{F \in \mathcal{F}_T} \|v\|_{0,F} \frac{|F|^{\frac{1}{2}}}{\int_F b_F^{\mathrm{c}}} \|b_F^{\mathrm{c}}\|_{0,T} \le c h_T^{\frac{1}{2}} \sum_{F \in \mathcal{F}_T} \|v\|_{0,F}.$$

(2) For $w \in H_0^1(\Omega)$,

$$\begin{aligned}\Lambda_h(u - u_h, w) &= \Lambda_h(u, w - \mathcal{I}_{\mathrm{BV}} w) + \Lambda_h(u, \mathcal{I}_{\mathrm{BV}} w) - \Lambda_h(u_h, w - \mathcal{I}_{\mathrm{BV}} w) - \Lambda_h(u_h, \mathcal{I}_{\mathrm{BV}} w) \\ &= (f, w - \mathcal{I}_{\mathrm{BV}} w)_{0,\Omega} + (f - f_h, \mathcal{I}_{\mathrm{BV}} w)_{0,\Omega} - \Lambda_h(u_h, \Pi(w - \mathcal{I}_{\mathrm{BV}} w)).\end{aligned}$$

Since $\widehat{u}_h$ is the solution of problem (4.2) and $\Pi(w - \mathcal{I}_{\mathrm{BV}} w) \in \mathcal{B}_{\mathrm{c}}(\mathcal{T}_h)$,

$$\begin{aligned}\Lambda_h(u - u_h, w) = (f, w - \mathcal{I}_{\mathrm{BV}} w)_{0,\Omega} &- (f_h, \Pi(w - \mathcal{I}_{\mathrm{BV}} w))_{0,\Omega} \\ &+ \Lambda_h(\widehat{u}_h, \Pi(w - \mathcal{I}_{\mathrm{BV}} w)) + (f - f_h, \mathcal{I}_{\mathrm{BV}} w)_{0,\Omega}.\end{aligned}$$

(3) The next step is to localize and upper bound the four terms in the right-hand side of the above equation. Owing to (3.1),

$$(f, w - \mathcal{I}_{\mathrm{BV}} w)_{0,T} \le c h_T \|f\|_{k^{-1};0,T} |w|_{k;1,\Delta_T}.$$

Furthermore, (3.2) and (4.22) yield

$$\begin{aligned}(f_h, \Pi(w - \mathcal{I}_{\mathrm{BV}} w))_{0,T} &\le c \|f_h\|_{0,T} h_T^{\frac{1}{2}} \sum_{F \in \mathcal{F}_T} \|w - \mathcal{I}_{\mathrm{BV}} w\|_{0,F} \\ &\le c h_T \|f_h\|_{0,T} \sum_{F \in \mathcal{F}_T} (k_F^{\star})^{-\frac{1}{2}} |w|_{k;1,\Delta_F} \le c h_T \|f_h\|_{k^{-1};0,T} \sum_{F \in \mathcal{F}_T} |w|_{k;1,\Delta_F}.\end{aligned}$$

Moreover, using (3.2) and (4.21) yields

$$k_T(\nabla\widehat{u}_h,\nabla\Pi(w-\mathcal{I}_{\rm BV}w))_{0,T}\le c\|\nabla\widehat{u}_h\|_{k;0,T}k_T^{\frac12}h_T^{-\frac12}\sum_{F\in\mathcal{F}_T}\|w-\mathcal{I}_{\rm BV}w\|_{0,F}$$

$$\le c|\widehat{u}_h|_{k;1,T}k_T^{\frac12}h_T^{-\frac12}\sum_{F\in\mathcal{F}_T}h_F^{\frac12}(k_F^\star)^{-\frac12}|w|_{k;1,\Delta_F}\le c|\widehat{u}_h|_{k;1,T}\sum_{F\in\mathcal{F}_T}|w|_{k;1,\Delta_F}.$$

Finally, using the stability property (3.18) established in Lemma 3.10, it is readily inferred that

$$(f-f_h,\mathcal{I}_{\rm BV}w)_{0,T}=(f-f_h,\mathcal{I}_{\rm BV}w-\Pi^0(\mathcal{I}_{\rm BV}w))_{0,T}\le ch_T\|f-f_h\|_{k^{-1};0,T}|\mathcal{I}_{\rm BV}w|_{k;1,T}$$

$$\le ch_T\|f-f_h\|_{k^{-1};0,T}|w|_{k;1,\Delta_T}.$$

Collecting the above estimates and using (4.11) yields

$$\Lambda_h(u-u_h,w)\le c\left(\sum_{F\in\mathcal{F}_h^i}\mathcal{P}_{3,F}(f)^2+\sum_{T\in\mathcal{T}_h}\mathcal{P}_{5,T}(f)^2\right)^{\frac12}|w|_{k;1,h}. \tag{4.23}$$

(4) Let $v_h\in P^1_{\mathrm{c},0}(\mathcal{T}_h)$ and let $w=u-v_h$. The estimate (4.18) is readily deduced from (4.23) and the identity $|w|^2_{k;1,h}=\Lambda_h(u-u_h,w)+\Lambda_h(u_h-v_h,w)$. □

Remark 4.14. If f is smooth, the second term in the right hand side of (4.19) is one order higher than the first.

The following results are a direct consequence of (3.4) and (4.18).

Corollary 4.15. *Let u and u_h be respectively the unique solution of* (1.4) *and* (2.6)*. Then, under Hypotheses* 3.1 *and* 3.7*, there exists a constant c such that*

$$|u-u_h|_{k;1,h}\le c\left(\sum_{F\in\mathcal{F}_h^i}\mathcal{P}_{3,F}(f)^2+\sum_{T\in\mathcal{T}_h}\mathcal{P}_{5,T}(f)^2+\sum_{T\in\mathcal{T}_h}\eta_{1,T}(u_h)^2\right)^{\frac12} \tag{4.24}$$

$$\le c\left(\sum_{F\in\mathcal{F}_h^i}\mathcal{P}_{3,F}(f)^2+\sum_{T\in\mathcal{T}_h}\mathcal{P}_{5,T}(f)^2+\sum_{F\in\mathcal{F}_h}\eta_{2,F}(u_h)^2\right)^{\frac12}. \tag{4.25}$$

Finally, we investigate the optimality of the above error indicators. Owing to Propositions 3.6 and 4.8, we only need to prove the optimality of $\mathcal{P}_{5,T}(f)$.

Proposition 4.16. *Let u and u_h be respectively the unique solution of* (1.4) *and* (2.6)*. Then, there exists a constant c such that*

$$\forall T\in\mathcal{T}_h,\quad \mathcal{P}_{5,T}(f)\le c\left(|u-u_h|_{k;1,T}+h_T\|f-f_h\|_{k^{-1};0,T}\right). \tag{4.26}$$

Proof. Classical techniques [12,32] show that for all $T\in\mathcal{T}_h$,

$$h_T\|f\|_{k^{-1};0,T}\le ch_T\left(\|f_h\|_{k^{-1};0,T}+\|f-f_h\|_{k^{-1};0,T}\right)\le c\left(|u-u_h|_{k;1,T}+h_T\|f-f_h\|_{k^{-1};0,T}\right),$$

yielding the desired result. □

Remark 4.17. It is not straightforward to construct a hierarchical *a posteriori* error estimator based on non-conforming element bubbles that circumvents the saturation assumption since the proof of Proposition 4.13 relies on the construction of an operator Π such that $\Lambda_h(v_h,v)=\Lambda_h(v_h,\Pi v)$ for all $v_h\in P^1_{\mathrm{nc},0}(\mathcal{T}_h)$ and $v\in H^1_0(\Omega)$. Indeed, if Πv is in $\mathcal{B}_{\rm nc}(\mathcal{T}_h)$, $\Lambda_h(v_h,\Pi v)=0$ owing to Lemma 4.9.

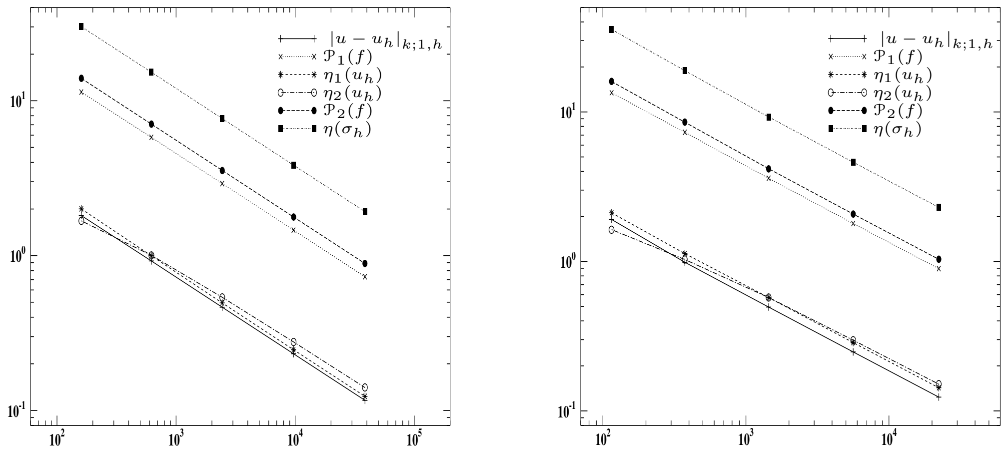

FIGURE 2. Actual error and residual error estimators as a function of the number of faces in the mesh. Left: quasi-uniform triangulations; right: non-uniform triangulations.

5. Numerical results

This section presents results illustrating the performance of the above residual and hierarchical estimators for homogeneous and heterogeneous media.

5.1. Homogeneous media

Consider the square $\Omega =]0,1[\times]0,1[$ with homogeneous Dirichlet boundary conditions and constant conductivity $k=1$. The data f is chosen so that the exact solution of (1.4) is $u(x,y) = \sin(2\pi x)\sin(2\pi y)$. Two families of unstructured triangulations are considered. The first family consists of quasi-uniform triangulations with mesh-size parameter $h_i = h_0 2^{-i}$, $h_0 = 0.2$ and $i \in \{0,\dots,4\}$. The second family is non-uniform with triangle size near the boundary as before whereas triangle sizes are ten times smaller in the vicinity of the point $(0.5, 0.5)$. Henceforth, error estimators and actual errors are plotted as a function of degrees of freedom for the primal formulation (2.6), *i.e.* the number of faces in the mesh, which in two dimensions, scales as the reciprocal of the square of the mesh-size.

Figure 2 presents results for the residual error estimators derived in Section 3. It displays the actual pressure error $|u-u_h|_{k;1,h}$, the pre-processing terms

$$\mathcal{P}_1(f) = \left(\sum_{T\in\mathcal{T}_h} \mathcal{P}_{1,T}(f)^2\right)^{\frac{1}{2}}, \qquad \mathcal{P}_2(f) = \left(\sum_{T\in\mathcal{T}_h} \mathcal{P}_{2,T}(f)^2\right)^{\frac{1}{2}}, \tag{5.1}$$

with local error indicators defined in (3.6) and (3.16), respectively, the post-processing terms

$$\eta_1(u_h) = \left(\sum_{T\in\mathcal{T}_h} \eta_{1,T}(u_h)^2\right)^{\frac{1}{2}}, \qquad \eta_2(u_h) = \left(\sum_{F\in\mathcal{F}_h} \eta_{2,F}(u_h)^2\right)^{\frac{1}{2}}, \tag{5.2}$$

with local error indicators defined in (3.9) and (3.10), respectively, and the velocity error estimator

$$\eta(\sigma_h) = \eta_2(u_h) + \mathcal{P}_1(f) + \mathcal{P}_2(f), \tag{5.3}$$

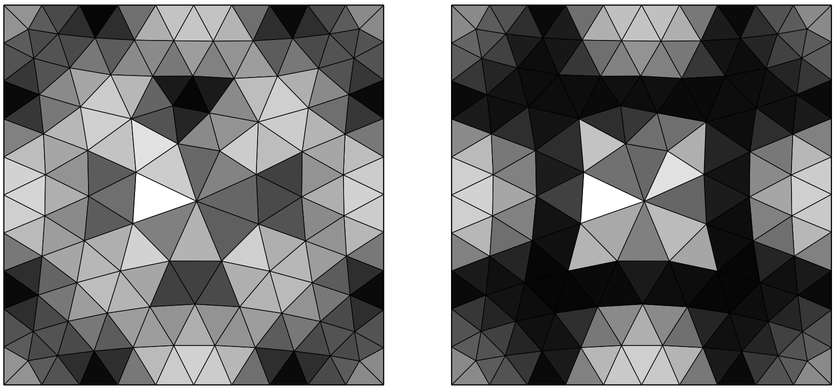

Figure 3. Actual error (left) and residual error estimator $\eta_1(u_h)$ (right) for the quasi-uniform triangulation with mesh-size parameter $h = \frac{h_0}{2}$.

resulting from Corollary 3.9 and Proposition 3.13 by setting the constants to one. All the quantities in (5.1) and (5.2) can be evaluated by performing one or two loops over the mesh elements; hence, their evaluation requires nearly the same cost, *i.e.*, a cost proportional to the number of degrees of freedom for the discrete pressure problem and, hence, much lower than that associated with the solution of the primal formulation (2.6). Figure 2 shows that the actual pressure error is first-order in the mesh size, in agreement with the *a priori* error analysis. Moreover, all the error estimators exhibit the correct order of convergence. Notice that the pre-processing terms $\mathcal{P}_1(f)$ and $\mathcal{P}_2(f)$ dominate the post-processing terms $\eta_1(u_h)$ and $\eta_2(u_h)$.

The effectivity indices for the pressure error estimators $\eta_i(u_h)$, $i \in \{1, 2\}$, defined as (see Cor. 3.9)

$$I_i = \frac{\eta_i(u_h) + \mathcal{P}_2(f)}{|u - u_h|_{k;1,h}}, \quad i \in \{1, 2\}, \tag{5.4}$$

are in the range 8.8 to 9.8. These quantities are close to 1 if the term $\mathcal{P}_2(f)$ is not included. The effectivity indices for the pressure-and-velocity error estimator based on the mixed formulation, defined as (see Cor. 3.4)

$$I_{2+i} = \frac{\eta_i(u_h) + \mathcal{P}_1(f)}{|u - u_h|_{k;1,h} + \|\sigma - \sigma_h\|_{k^{-1};\mathrm{div},\Omega}}, \quad i \in \{1, 2\}, \tag{5.5}$$

are in the range 0.85 to 0.87. Finally, the effectivity indices for the velocity error estimator based on the primal formulation, defined as (see Cor. 3.9 and Prop. 3.13)

$$I_{4+i} = \frac{\eta_i(u_h) + \mathcal{P}_1(f) + \mathcal{P}_2(f)}{\|\sigma - \sigma_h\|_{k^{-1};\mathrm{div},\Omega}}, \quad i \in \{1, 2\}, \tag{5.6}$$

are in the range 1.7 to 1.8, indicating that the actual velocity error approximately coincides with $\mathcal{P}_1(f)$. Thus, for homogeneous media, the velocity error estimator based on the mixed formulation yields sharper bounds than that based on the primal formulation and the local reconstruction formula (2.8).

To illustrate the optimality of the residual error estimators, Figure 3 presents the local pressure error $\|u - u_h\|_{k;1,T}$ and the local error indicators $\eta_{1,T}(u_h)$ on each triangle T of the quasi-uniform triangulation with mesh-size parameter $h = \frac{h_0}{2}$. The spatial distributions of both quantities exhibit similar features, in particular the localization of the maxima.

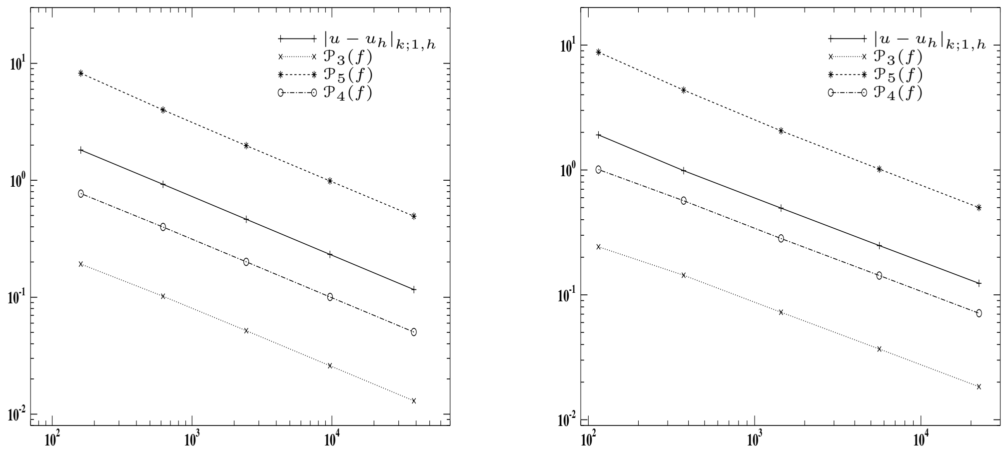

FIGURE 4. Actual error and hierarchical error estimators as a function of the number of faces in the mesh. Left: quasi-uniform triangulations; right: non-uniform triangulations.

Figure 4 presents results for the hierarchical error estimators derived in Section 4. It displays the actual pressure error and the pre-processing terms

$$\mathcal{P}_3(f) = \left(\sum_{F\in\mathcal{F}_h^i} \mathcal{P}_{3,F}(f)^2\right)^{\frac{1}{2}}, \qquad \mathcal{P}_4(f) = \left(\sum_{T\in\mathcal{T}_h} \mathcal{P}_{4,T}(f)^2\right)^{\frac{1}{2}}, \qquad \mathcal{P}_5(f) = \left(\sum_{T\in\mathcal{T}_h} \mathcal{P}_{5,T}(f)^2\right)^{\frac{1}{2}}, \tag{5.7}$$

with local error indicators defined in (4.10), (4.17), and (4.19), respectively. In all cases, the correct order of convergence is obtained. For nonconforming element bubbles, the saturation assumption has been verified numerically; the constant β was found to be equal to 0.82 for the quasi-uniform meshes and to 0.84 for the non-uniform meshes, thereby confirming that the saturation assumption is satisfied in this case. Although the saturation assumption cannot be guaranteed theoretically for conforming face bubbles, we notice that the estimator $\mathcal{P}_3(f)$ performs well for both quasi-uniform and non-uniform meshes. For the two estimators relying on the saturation assumption, the effectivity indices for the pressure error indicator, defined as (see Prop. 4.5 and 4.10)

$$I_{6+i} = \frac{\mathcal{P}_{2+i}(f)}{|u-u_h|_{k;1,h}}, \quad i\in\{1,2\}, \tag{5.8}$$

are in the range 0.1 to 0.4 independently of h. The estimator $\mathcal{P}_3(f)+\mathcal{P}_5(f)+\eta_i(u_h)$, $i\in\{1,2\}$, resulting from Proposition 4.13 has the theoretical advantage of circumventing the saturation assumption, but its effectivity index is in the range 5.3 to 6.0.

5.2. **Heterogeneous media**

Consider the square $\Omega =]-1,1[\times]-1,1[$ with homogeneous Dirichlet boundary conditions. The domain Ω is split into $L=4$ four square subdomains Ω_l with sides of length 1. Subdomains are numbered counterclockwise starting with the upper right one. On each subdomain Ω_l, $l\in\{1,\ldots,4\}$, the conductivity is set to $k_l=\kappa^{l-1}$. Observe that the variations of k are compatible with Hypothesis 3.1. Owing to the particular arrangement of the subdomains where each Ω_l has a non-empty intersection with the boundary of Ω, one can verify from the proof of Proposition 2.2 that the quantity $\varrho_\Omega(k)$ no longer appears in the inf-sup constant associated with the bilinear form B. As a result, the pressure-and-velocity error estimator based on the mixed

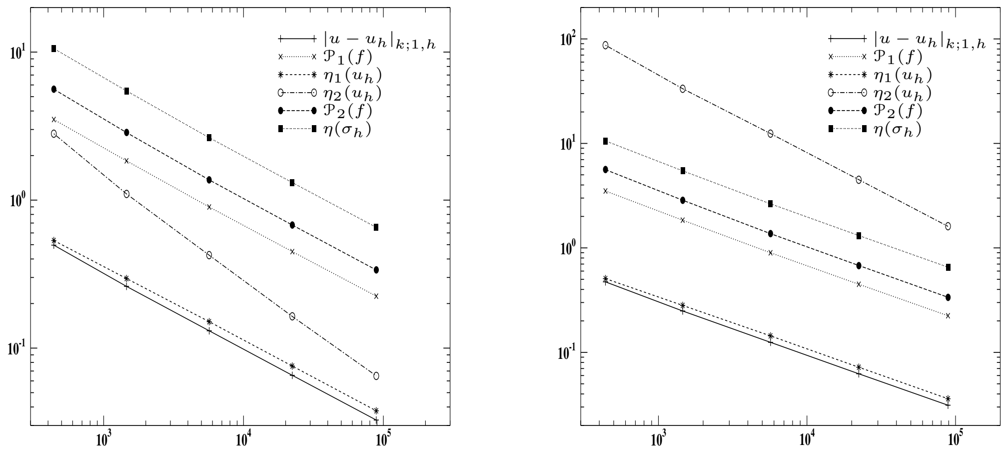

FIGURE 5. Actual error and residual error estimators as a function of the number of faces in the mesh. Left: $\varrho_\Omega(k) = 10^3$; right: $\varrho_\Omega(k) = 10^6$.

formulation does not depend on $\varrho_\Omega(k)$; however, the local lower bounds involving $\eta_{1,T}(u_h)$ and $\eta_{2,F}(u_h)$ still depend on $\varrho_F(k)$. We consider two values for the parameter κ: $\kappa = 10$ yielding a maximum contrast in the conductivity of $\varrho_\Omega(k) = 10^3$; $\kappa = 100$ yielding a maximum contrast in the conductivity of $\varrho_\Omega(k) = 10^6$. In both cases, the data is $f(x, y) = 2\pi^2 \sin(\pi x) \sin(\pi y)$ so that on each subdomain Ω_l, the exact solution is $u(x, y)|_{\Omega_l} = \frac{1}{k_l} \sin(\pi x) \sin(\pi y)$. Note that the exact solution exhibits a $\mathcal{C}^1$ singularity at the interfaces between subdomains.

Results are presented on a family of quasi-uniform, unstructured triangulations with mesh-size parameter $h_i = h_0 2^{-i}$, $h_0 = 0.2$ and $i \in \{0, \ldots, 4\}$. The triangulations are always compatible with the subdomains Ω_l, in agreement with Hypothesis 2.4. Figure 5 presents the actual pressure error as well as the same residual error estimators as in Figure 2. The left plot in Figure 5 deals with the case $\varrho_\Omega(k) = 10^3$ and the right plot with the case $\varrho_\Omega(k) = 10^6$. In all cases the correct order of convergence is obtained except for $\eta_2(u_h)$ which exhibits super-convergence. The values taken by $\eta_2(u_h)$ are larger when $\varrho_\Omega(k) = 10^6$ since the pressure jumps are maximal at the subdomain interfaces where the face-averaged conductivity $\{k\}_F$ can be very large. Moreover, no degradation in the effectivity indices is observed when going from $\varrho_\Omega(k) = 10^3$ to $\varrho_\Omega(k) = 10^6$. This confirms that the various pressure error estimators are independent of the fluctuations in k.

Figure 6 presents the same hierarchical error estimators as in Figure 4. The same conclusions as for the residual error estimators can be drawn. Our results show in particular that, for the present test cases, the saturation constant β does not depend on $\varrho_\Omega(k)$.

5.3. **Adaptive mesh refinement**

This section briefly illustrates how the above error indicators can be used to construct adaptively refined meshes. For conciseness, we consider only the heterogeneous case discussed in the previous section with $\varrho_\Omega(k) = 10^3$, and use the local error indicators $\eta_{1,T}(u_h)$ to refine the mesh adaptively. The refinement algorithm is the following:

(i) Construct an initial mesh $\mathcal{T}_h^0$. Set $i = 0$.
(ii) Solve the discrete problem (2.6) on $\mathcal{T}_h^i$. Let u_h^i denote its solution.
(iii) Calculate the local error indicators $\eta_{1,T^i}(u_h^i)$ on each $T^i \in \mathcal{T}_h^i$.

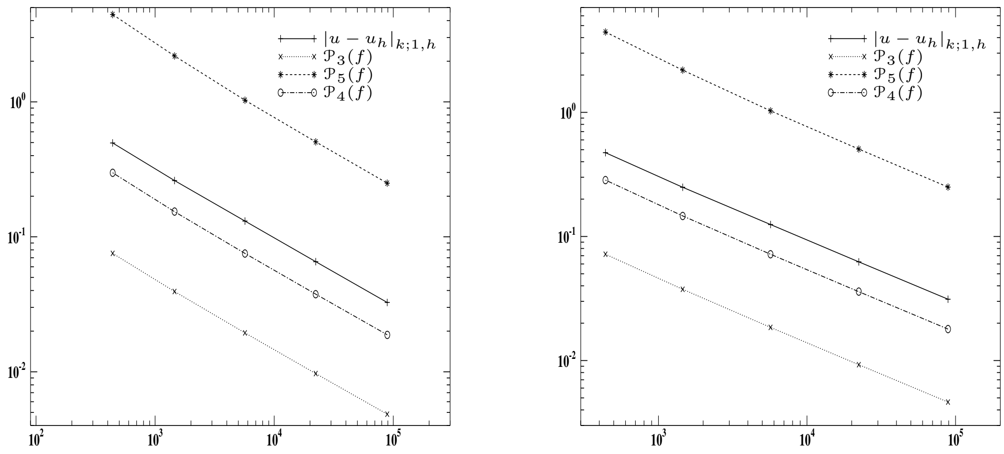

FIGURE 6. Actual error and hierarchical error estimators as a function of the number of faces in the mesh. Left: $\varrho_\Omega(k) = 10^3$; right: $\varrho_\Omega(k) = 10^6$.

(iv) Calculate the size $h_{T^{i+1}}$ of the triangles of the new mesh from the local error indicators $\eta_{1,T^i}(u_h^i)$,

$$h_{T^{i+1}} = l(\eta_{T^i}(u_h^i))\, h_{T^i}, \qquad l(\eta_{T^i}(u_h^i)) = \begin{cases} \frac{1}{2} & \text{if } \eta_{T^i}(u_h^i) \geq \text{Tol}, \\ 1 & \text{otherwise}, \end{cases} \tag{5.9}$$

where $\text{Tol} = \frac{1}{2\,nt^i} \sum_{T^i \in \mathcal{T}_h^i} \eta_{1,T^i}(u_h^i)$ and nt^i is the number of triangles in $\mathcal{T}_h^i$.

(v) Construct the next mesh $\mathcal{T}_h^{i+1}$ using a Delaunay mesh generator and return to step (ii).

Figures 7 shows the initial mesh and the mesh generated by the above algorithm after 6 iterations. We observe that the mesh is refined along the interfaces of subdomains, particularly along the interface between subdomains Ω_1 and Ω_4, across which the jump of the coefficient k is maximal. The adaptively refined mesh, which has 54 738 faces, does not contain hanging nodes at the interfaces. On this mesh, the actual pressure error $|u - u_h|_{k;1,h}$ is 0.041; on the finest, uniformly refined mesh considered in the previous section, this error is only slightly lower, 0.033, but the mesh contains 88 961 faces. Moreover, the actual pressure error exhibits the optimal $\frac{1}{2}$-order convergence in the number of mesh faces on the present sequence of adaptively refined meshes. Finally, we verified numerically that the saturation assumption holds for nonconforming element bubbles, whereas for conforming face bubbles, if the saturation assumption holds, the constant β is estimated to be larger than 0.8.

6. Conclusions

In this paper we have presented a mathematical analysis of residual and hierarchical *a posteriori* error estimates for nonconforming finite element approximations of elliptic problems with variable coefficients. Particular attention was devoted to obtaining global upper and local lower bounds for the discretization errors valid for strongly heterogeneous media, such as those encountered in applications dealing with subsurface flows. All the error estimators have been assessed numerically on test cases with constant, varying, and strongly varying coefficients, and an example illustrating how the error estimators can be localized to generate adaptively refined meshes has been presented.

From a practical standpoint, the following conclusions can be drawn. All the residual and hierarchical estimators can be evaluated at approximately the same computational cost, which is proportional to the degrees of freedom; this cost is significantly lower than that associated with the solution of the primal formulation (2.6).

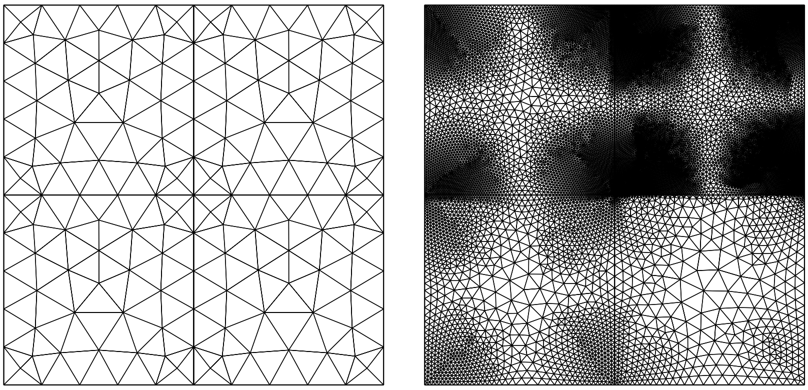

FIGURE 7. Left: initial mesh (440 faces); right: adaptively refined mesh (54 738 faces).

The hierarchical estimators relying on a saturation assumption only involve pre-processing terms, but the difficulty associated with these estimators is that the saturation assumption may not hold. Using conforming face bubbles, a hierarchical estimator circumventing the saturation assumption has been derived. This estimator is sharper than the residual estimator based on the primal formulation. Both estimators involve a conforming reconstruction of the discrete pressure; an efficient way to achieve this is to use the Oswald interpolation operator, leading to the element-oriented error indicators $\eta_{1,T}(u_h)$. These estimators are sharper than the face-oriented error indicators $\eta_{2,F}(u_h)$ and are, therefore, recommended for practical evaluations. Furthermore, for the present test cases, it has been observed that the error indicators $\eta_{1,T}(u_h)$ alone (*i.e.*, without the addition of the pre-processing terms required by the theory) can be effectively used to track the pressure error and to generate adaptively refined meshes. Finally, velocity error estimators based on the mixed formulation are sharper than those based on the primal formulation and the local velocity reconstruction; however, the former can depend on the fluctuations of the coefficient k, but not the latter.

Acknowledgements. This work was supported in part by the GdR MoMaS (CNRS–2439, ANDRA, BRGM, CEA, EdF). The authors are thankful to C. Bernardi (Université Paris VI, France) and J.-P. Croisille (Université de Metz, France) for fruitful discussions and also to an anonymous referee for several valuable suggestions.

References

[1] B. Achchab, S. Achchab and A. Agouzal, Hierarchical robust *a posteriori* error estimator for a singularly pertubed problem. *C.R Acad. Paris I* **336** (2003) 95–100.

[2] B. Achchab, A. Agouzal, J. Baranger and J.F. Maitre, Estimateur d'erreur *a posteriori* hiérarchique. Application aux éléments finis mixtes. *Numer. Math.* **80** (1998) 159–179.

[3] Y. Achdou and C. Bernardi, Un schéma de volumes ou éléments finis adaptatif pour les équations de Darcy à perméabilité variable. *C.R Acad. Paris I* **333** (2001) 693–698.

[4] Y. Achdou, C. Bernardi and F. Coquel, *A priori* and *a posteriori* analysis of finite volume discretizations of Darcy's equations. *Numer. Math.* **96** (2003) 17–42.

[5] M. Ainsworth and J.T. Oden, *A posteriori error estimation in finite element analysis.* Wiley-Interscience Publication (2000).

[6] L. Angermann, *A posteriori* error estimates for FEM with violated Galerkin orthogonality. *Numer. Methods Partial Differential Equations* **18** (2002) 241–259.

[7] D.N. Arnold and F. Brezzi, Mixed and nonconforming finite element methods: implementation, postprocessing and error estimates. *RAIRO Modél. Math. Anal. Numér.* **19** (1985) 7–32.

[8] R. Bank and K. Smith, *A posteriori* estimates based on hierarchical bases. *SIAM J. Numer. Anal.* **30** (1991) 921–935.

[9] R.E. Bank and A. Weiser, Some *a posteriori* error estimators for elliptic partial differential equations. *Math. Comp.* **44** (1985) 283–301.

[10] R. Becker, P. Hansbo and M.G. Larson, Energy norm *a posteriori* error estimation for discontinuous Galerkin methods. *Comput. Methods Appl. Mech. Engrg.* **192** (2003) 723–733.

[11] C. Bernardi, private communication.

[12] C. Bernardi and R. Verfürth, Adaptive finite element methods for elliptic equations with non-smooth coefficients. *Numer. Math.* **85** (2000) 579–608.

[13] D. Braess, *Finite elements*. Cambridge Univ. Press (1997).

[14] C. Carstensen, *A posteriori* error estimate for the mixed finite element method. *Math. Comp.* **66** (1997) 465–476.

[15] C. Carstensen and A. Funken, *A posteriori* error control in low-order finite element discretizations of incompressible stationary flow problems. *Math. Comp.* **70** (2000) 1353–1381.

[16] B. Courbet and J.-P. Croisille, Finite volume box schemes on triangular meshes. *RAIRO Modél. Math. Anal. Numér.* **32** (1998) 631–649.

[17] J.-P. Croisille, Finite volume box schemes and mixed methods. *ESAIM: M2AN* **31** (2000) 1087–1106.

[18] J.-P. Croisille and I. Greff, Some nonconforming mixed box schemes for elliptic problems. *Numer. Methods Partial Differential Equations* **8** (2002) 355–373.

[19] M. Crouzeix and P.-A. Raviart, Conforming and nonconforming mixed finite element methods for solving the stationary Stokes equations I. *RAIRO Anal. Numér.* **3** (1973) 33–75.

[20] E. Dari, R. Durán and C. Parda, Error estimators for nonconforming finite element approximations of the Stokes problem. *Math. Comp.* **64** (1995) 1017–1033.

[21] E. Dari, R. Durán, C. Parda and V. Vampa, *A posteriori* error estimators for nonconforming finite element methods. *RAIRO Modél Math. Anal. Numér.* **30** (1996) 385–400.

[22] A. Ern and J.-L. Guermond, *Theory and practice of finite elements*, *Appl. Math. Ser.*, Springer, New York **159** (2004).

[23] M. Fortin and M. Soulié, A non-conforming piecewise quadratic finite element on triangles. *Int. J. Num. Meth. Engrg.* **19** (1983) 505–520.

[24] R.H.W. Hoppe and B. Wohlmuth, Element-oriented and edge-oriented local error estimators for non-conforming finite element methods. *RAIRO Modél. Math. Anal. Numér.* **30** (1996) 237–263.

[25] V. John, *A posteriori* L^2-error estimates for the nonconforming P_1/P_0-finite element discretization of the Stokes equations. *J. Comput. Appl. Math.* **96** (1998) 99–116.

[26] G. Kanschat and F.-T. Suttmeier, *A posteriori* error estimates for non-conforming finite element schemes. *Calcolo* **36** (1999) 129–141.

[27] O. Karakashian and F. Pascal, *A posteriori* error estimates for a discontinuous Galerkin approximation of second order elliptic problems. *SIAM J. Numer. Anal.* **41** (2003) 2374–2399.

[28] P.-A. Raviart and J.-M. Thomas, A mixed finite element method for second order elliptic problems, in *Mathematical Aspects of the Finite Element Method*, E. Magenes and I. Galligani Eds., Springer-Verlag, New York, *Lect. Notes Math.* **606** (1977).

[29] F. Schieweck, *A posteriori* error estimates with post-processing for nonconforming finite elements. *ESAIM: M2AN* **36** (2002) 489–503.

[30] J.-M. Thomas and D. Trujillo, Mixed finite volume methods. *Int. J. Num. Meth. Engrg.* **46** (1999) 1351–1366.

[31] R. Verfürth, *A posteriori* error estimators for the Stokes equations. II. Non-conforming discretizations. *Numer. Math.* **60** (1991) 235–249.

[32] R. Verfürth, *A review of a posteriori error estimation and adaptative mesh-refinement techniques*. Chichester, England (1996).

[33] B.I. Wohlmuth and R.H.W. Hoppe, A comparison of *a posteriori* error estimators for mixed finite element discretizations by Raviart-Thomas. *Math. Comp.* **68** (1999) 1347–1378.